

Davidson Y, Ahmed Z, Holton J, Thompson JC, Akiyama H, Arai T, Hasegawa M, Gerhard A, Allsop and Mann DM	fluid α -synuclein levels are raised in multiple system atrophy and distinguish this from the other α -synucleinopathies, Parkinson's disease and Dementia with Lewy bodies.				
Hasegawa M, Nonaka T, Tsuji H, Tamaoka A, Yamashita M, Kametani F, Yoshida M, Arai T, Akiyama H	Molecular Dissection of TDP-43 Proteinopathies.	J Mol Neurosci	45	480-485	2011
Nonaka T and Hasegawa M	In vitro recapitulation of aberrant protein inclusions in neurodegenerative diseases, New cellular models of neurodegenerative diseases.	Commun & Integ Biol	4	501-502	2011
Meyerowitz J, Parker SJ, Vella LJ, Ng DCh, Price KA, Liddell JR, Caragounis A, Li QX, Masters CL, Nonaka T, Hasegawa M, Bogoyevitch MA, Kanninen KM, Crouch PJ, White AR	C-Jun N-terminal kinase controls TDP-43 accumulation in stress granules induced by oxidative stress.	Mol Neurodegener	6	57	2011
長谷川成人, 新井哲明, 野中隆, 亀谷富由樹, 秋山治彦	病理構造物の解析からみちびかれた精神神経疾患の新しい考え方.	精神医学,	53	1201-1206	2011

鈴掛雅美, 長谷川成人	: 認知症学, 神経原線維変化の形成と分布.	日本臨床,	69	148-152	2011
團彩帆, 長谷川成人:	認知症学, FTDP-17の分子生物学.	日本臨床,	69	379-383	2011

IV.研究成果の刊行物・別刷

Lipoprotein Lipase Is a Novel Amyloid β ($A\beta$)-binding Protein That Promotes Glycosaminoglycan-dependent Cellular Uptake of $A\beta$ in Astrocytes^{*[5]}

Received for publication, August 4, 2010, and in revised form, November 23, 2010. Published, JBC Papers in Press, December 21, 2010, DOI 10.1074/jbc.M110.172106

Kazuchika Nishitsuji[‡], Takashi Hosono[‡], Kenji Uchimura^{‡§}, and Makoto Michikawa^{‡1}

From the [§]Section of Pathophysiology and Neurobiology, [‡]Department of Alzheimer's Disease Research, National Center for Geriatrics and Gerontology, Obu, Aichi 474-8511, Japan

Lipoprotein lipase (LPL) is a member of a lipase family known to hydrolyze triglyceride molecules in plasma lipoprotein particles. LPL also plays a role in the binding of lipoprotein particles to cell-surface molecules, including sulfated glycosaminoglycans (GAGs). LPL is predominantly expressed in adipose and muscle but is also highly expressed in the brain where its specific roles are unknown. It has been shown that LPL is colocalized with senile plaques in Alzheimer disease (AD) brains, and its mutations are associated with the severity of AD pathophysiological features. In this study, we identified a novel function of LPL; that is, LPL binds to amyloid β protein ($A\beta$) and promotes cell-surface association and uptake of $A\beta$ in mouse primary astrocytes. The internalized $A\beta$ was degraded within 12 h, mainly in a lysosomal pathway. We also found that sulfated GAGs were involved in the LPL-mediated cellular uptake of $A\beta$. Apolipoprotein E was dispensable in the LPL-mediated uptake of $A\beta$. Our findings indicate that LPL is a novel $A\beta$ -binding protein promoting cellular uptake and subsequent degradation of $A\beta$.

Lipoprotein lipase (LPL)² catalyzes the hydrolysis of triacylglycerol and mediates the cellular uptake of lipoproteins by functioning as a "bridging molecule" between lipoproteins and sulfated glycosaminoglycans (GAGs) or lipoprotein receptors in blood vessels (1, 2). Sulfated GAGs are side chains of proteoglycans normally found in the extracellular matrix and on the cell surface in the peripheral tissues and brain. Sulfation modifications vary within the GAG chains and are

crucial for interaction between GAGs and various protein ligands (3), including LPL (4, 5).

It has been shown that LPL is distributed in numerous organs and is highly expressed in the brain (6, 7). Although the catabolic activity of LPL on triacylglycerol is observed in the brain (8), the finding that apolipoprotein CII (apoCII), an essential cofactor for LPL, is not expressed in the brain (9, 10), suggests that LPL has a novel nonenzymatic function in the brain. However, little is known about LPL function in the brain. Interestingly, it has been shown that LPL is accumulated in senile plaques of Alzheimer disease (AD) brains (11). Moreover, SNPs in the coding region of the LPL gene are associated with disease incidence in clinically diagnosed AD subjects, LPL mRNA expression level, brain cholesterol level, and the severity of AD pathologies, including neurofibrillary tangles and senile plaque density (12). These results suggest that LPL may have a physiological role in the brain, whose alternation is associated with the pathogenesis of AD.

The occurrence of senile plaques in the brain is one of the pathological hallmarks of AD. They contain extracellular deposits of amyloid β protein ($A\beta$), and the abnormal $A\beta$ deposition or the formation of soluble $A\beta$ oligomers is crucial for AD pathogenesis. $A\beta$ is a physiological peptide whose main species are 40 and 42 amino acids in length, and $A\beta$ 42 is the predominant species in senile plaques (13). The $A\beta$ levels are determined by the balance between its production and degradation/clearance, and an attenuated $A\beta$ catabolism is suggested to cause $A\beta$ accumulation in aging brains (14). Previous studies have shown that astrocytes and microglia directly take up and degrade $A\beta$ 42 (15, 16) and that $A\beta$ degradation occurs in late endosomal-lysosomal compartments (17, 18). These lines of evidence, together with the finding that LPL mediates the cellular uptake of lipoproteins (1, 2), led us to carry out experiments to determine whether LPL interacts with $A\beta$ to promote $A\beta$ cellular uptake and degradation in astrocytes. Here, we provide evidence that LPL forms a complex with $A\beta$ and facilitates $A\beta$ cell surface binding and uptake in mouse primary astrocytes through a mechanism that is dependent on heparan sulfate and chondroitin sulfate GAG chains, leading to the lysosomal degradation of $A\beta$.

MATERIALS AND METHODS

Materials—Bovine LPL, heparinases, and a polyclonal anti-actin antibody were purchased from Sigma. Synthetic $A\beta$ 1–42 was purchased from the Peptide Institute (Osaka,

* This work was supported by a grant-in-aid for scientific research on priority areas (Research on Pathomechanisms of Brain Disorders) from the Ministry of Education, Culture, Sports, Science, and Technology of Japan, a grant from the Program for Promotion of Fundamental Studies in Health Sciences of the National Institute of Biomedical Innovation, a grant from the Ministry of Health, Labor, and Welfare of Japan (Research on Dementia, Health, and Labor Sciences Research Grant H20-007), and a grant from the Japan Health Sciences Foundation (Research on Publicly Essential Drugs and Medical Devices).

[5] The on-line version of this article (available at <http://www.jbc.org>) contains supplemental "Methods" and Fig. 1.

¹ To whom correspondence should be addressed: Department of Alzheimer's Disease Research, National Center for Geriatrics and Gerontology, Gengo 35, Morioka, Obu, Aichi 474-8511, Japan. Tel.: 81-562-46-2311; Fax: 81-562-46-8569; E-mail: michi@ncgg.go.jp.

² The abbreviations used are: LPL, lipoprotein lipase; $A\beta$, amyloid β ; ApoE, apolipoprotein E; CS, chondroitin sulfate(s); HS, heparan sulfate; GAG, glycosaminoglycan; ANOVA, one-way analysis of variance.

LPL Promotes A β Cellular Uptake

Japan). Heparin, chondroitin, chondroitin sulfates, and chondroitinase ABC were from Seikagaku (Tokyo, Japan). Monoclonal anti-A β antibodies (6E10, 4G8) were purchased from Signet Laboratories (Dedham, MA), and a goat polyclonal anti-ApoE antibody and mouse control IgG were from Millipore (Bedford, MA). An anti-LPL antibody and Cy3- and FITC- conjugated secondary antibodies were purchased from Abcam, Inc. (Cambridge, MA). A monoclonal anti-A β antibody (2C8) was purchased from Medical and Biological Laboratories (Nagoya, Japan).

Animals—C57BL/6 mice were purchased from SLC, Inc. (Hamamatsu, Japan). ApoE-KO mice were obtained from Jackson ImmunoResearch Laboratories (Bar Harbor, ME). The National Center of Geriatrics and Gerontology Institutional Animal Care and Use Committee approved the animal studies.

Preparation of LPL—Because the sequence of LPL is highly conserved among mammalian species and the ability of LPL to interact with proteoglycans is also well conserved, we used LPL purified from bovine milk. An LPL suspension (suspended in 3.8 M ammonium sulfate, 0.02 M Tris-HCl, pH 8.0) was centrifuged ($10,000 \times g$ for 20 min at 4 °C), and the resulting pellet was dissolved in PBS. The prepared LPL was stored at 4 °C and used within 3 days.

Cell Culture—Highly astrocyte-rich cultures were prepared according to a method described previously (19). In brief, brains of postnatal day 2 C57BL/6 mice or ApoE knock-out mice were removed under anesthesia. The cerebral cortices from the mouse brains were dissected, freed from meninges, and diced into small pieces; the cortical fragments were incubated in 0.25% trypsin and 20 mg/ml DNase I in PBS at 37 °C for 20 min. The fragments were then dissociated into single cells by pipetting. The dissociated cells were seeded in 75-cm² dishes at a density of 5×10^7 cells per flask in DMEM-containing 10% FBS. After 10 days of incubation *in vitro*, flasks were shaken at 37 °C overnight, and the remaining astrocytes in the monolayer were trypsinized (0.1%) and reseeded. The astrocyte-rich cultures were maintained in DMEM-containing 10% FBS until use.

Assay of A β Binding and Uptake in Astrocytes by Western Blotting—Assays were carried out on confluent monolayers of astrocytes grown in 12-well plates. A β was dissolved in dimethyl sulfoxide to a final concentration of 1 mM and stored at -40 °C. A β (500 nM) and LPL (1–10 μ g/ml) were mixed in DMEM. Immediately, the mixture was added to the culture medium of astrocytes. Cells were incubated at 37 °C for 5 h to assess the cellular uptake of A β or at 4 °C for 3 h to evaluate the binding of A β to the cell surface of astrocytes. In these assays, cells were incubated in serum-free DMEM. After incubation, cells were washed with PBS three times, harvested using a cell scraper and lysed by sonication in radioimmune precipitation assay buffer (1% Nonidet P-40, 0.5% sodium deoxycholate, 0.1% SDS, 150 mM NaCl, 50 mM Tris-HCl (pH 8.0), 1 mM EDTA). Cell lysates were subjected to SDS-PAGE with 4–20% gradient gels (WAKO Pure Chemicals, Osaka, Japan) and transferred to polyvinylidene difluoride membranes (Millipore). A β was probed with 6E10 antibody followed by horseradish peroxidase-labeled anti-mouse antibody

(Cell Signaling Technology, Inc., Beverly, MA) and chemiluminescent substrate ECL Plus (GE Healthcare). The protein contents of cell lysates were normalized to the expression level of actin protein. To examine the involvement of GAGs, heparin, chemically modified heparins, chondroitin, or chondroitin sulfates (3 μ g/ml) were incubated with a mixture solution of A β and LPL. Astrocytes were pretreated with a mixture of heparinase II and heparinase III or chondroitinase ABC (0.03 units/ml) for 24 h at 37 °C to evaluate endogenously expressed glycosaminoglycans. Signals were visualized and quantified using a LAS-3000 luminescent image analyzer (Fujifilm, Tokyo, Japan) and ImageJ software (National Institutes of Health, Bethesda, MD). For analyzing protein band densities, a region of interest was drawn around a band, and protein band densities were calculated.

siRNA Interference of LPL—siRNA specific for mouse LPL (sense strand, 5'-CAGCUGAGGACACUUGUCAUCUCAUdTdT-3'; antisense strand, 5'-AUGAGAUGACAAGUGUCCUCAGCUGdTdT-3') and control siRNA (sense strand, 5'-CAGAGGGCACAUUUGACCUUCCAUCdTdT-3'; antisense strand, 5'-AUGGAAAGGUCAAAUGUGCCCUCUG-3') was purchased from Invitrogen. Astrocytes grown in 12-well plates for 24 h were transfected with either LPL siRNA or control siRNA with Lipofectamine RNAiMAX (Invitrogen). Forty-eight hours after transfection, cells were treated with A β (1 μ M) and then incubated at 4 °C for 3 h, and cell-surface associated A β was analyzed as described above. An anti-LPL antibody (Gene Tex, Inc.) was used for the detection of LPL.

Assay of A β Degradation in Astrocytes—Astrocytes were incubated with A β (250 nM) and LPL (2 μ g/ml) at 37 °C for 5 h. Subsequently, cells were washed with DMEM and incubated in DMEM for additional hours. Then, A β in cell lysates was analyzed by Western blotting as described above.

Immunoprecipitation—A β (500 nM) and LPL at various concentrations were incubated in DMEM at 37 °C for 3 h. LPL-A β complexes were immunoprecipitated with an anti-LPL antibody and magnetic protein G beads (Dyna, Hamburg, Germany). For detection of LPL-A β complexes in the mice brains, brain homogenates from 12-week-old C57BL/6 mice were used. In brief, anesthetized mice were perfused with PBS containing 35 μ g/ml heparin for 15 min. The cerebrum was dissected out and homogenized by sonication in 4 volumes of PBS containing a protease inhibitor mixture (P8340; Sigma) and centrifuged at $1,000 \times g$ for 10 min at 4 °C. The supernatants were harvested and LPL-A β complexes were immunoprecipitated with an anti-LPL antibody and magnetic protein G beads. The obtained precipitates were washed three times with PBS and incubated at 70 °C for 10 min in SDS sample buffer. Dissociated A β recovered in the supernatant was assessed by Western blotting as described above. For detection of endogenous A β , the supernatants were subjected to SDS-PAGE with 4–20% gradient gels and transferred to polyvinylidene difluoride membranes. The membranes were exposed to microwave irradiation for 20 s, and A β was probed with 4G8 antibody followed by horseradish peroxidase-labeled anti-mouse antibody and the chemiluminescent substrate ECL Plus.

LPL Promotes A β Cellular Uptake

Immunocytochemistry—Astrocytes grown on poly-L-lysine-coated coverslips were incubated with a mixture of A β (250 nM) and LPL (2 μ g/ml) at 37 °C for 5 h. After treatment, the cells were fixed with 4% paraformaldehyde in PBS at room temperature for 10 min, blocked, and permeabilized with 10% normal goat serum and 0.05% saponin in PBS at room temperature for 20 min. In some experiments, cells were washed twice with DMEM followed by incubation at 37 °C for 3 h in DMEM and fixed. The cells were then incubated with primary antibodies followed by Cy3- and FITC-conjugated secondary antibodies. The stained specimens were mounted with Fluor-Save reagents (Calbiochem) and examined under an LSM 510 confocal laser microscope (Carl Zeiss MicroImaging GmbH, Jena, Germany).

Statistical Analysis—The collected data were analyzed by one-way analysis of variance (ANOVA) including appropriate variables followed by the Dunnett's test or unpaired Student's *t* test. Results were considered significant when *p* < 0.05.

RESULTS

LPL Binds to A β *in Vitro*—LPL was incubated with freshly prepared A β 42 *in vitro*, and the complexes formed were immunoprecipitated with an anti-LPL antibody coupled with magnetic beads, followed by probing Western blots of protein complexes using an anti-A β antibody (Fig. 1A). A β 42 was immunoprecipitated with an anti-LPL antibody, but not with control IgG. The levels of A β 42 recovered in the immunoprecipitates from samples in the presence of 2–5 μ g/ml LPL were significantly higher than those from samples in the presence of 0, 0.5, or 1 μ g/ml of LPL (Fig. 1, B and C), suggesting that LPL directly interacts with A β 42, and these two molecules form a complex in an LPL dose-dependent manner. Furthermore, endogenous mouse A β was immunoprecipitated with the anti-LPL antibody from brain homogenates prepared from C57BL/6 mice (Fig. 1D), indicating that endogenous mouse LPL directly interacts with endogenous mouse A β . We also determined the assembly state of A β that forms complex with LPL. Solutions containing A β oligomers were subjected to immunoprecipitation/immunoblot analysis, and A β 42 monomers were immunoprecipitated by an anti-LPL antibody (supplemental Fig. 1).

LPL Promotes Cell Surface Binding and Cellular Uptake of A β in Astrocytes—We then determined whether LPL affects the cellular binding of A β to astrocytes. Soluble A β 42 and various concentrations of LPL were added to primarily cultured astrocytes prepared from WT mice and then incubated at 4 °C. LPL (2–5 μ g/ml) significantly augmented A β 42 binding to astrocytes by 5.8- to 9-fold of that in the case without LPL (Fig. 2, A and B). To examine the effect of LPL on the cellular uptake of A β , we incubated primary astrocytes with soluble A β 42 at 37 °C for 5 h. Apparently, the level of A β uptake by astrocytes increased in the presence of LPL at concentrations of 2 to 5 μ g/ml (Fig. 2C, lysate). Consistent with the increase in the level of cellular uptake of A β , the level of A β remaining in culture medium was decreased (Fig. 2C, medium). The A β levels in the cell lysate quantified are shown in Fig. 2D, indicating that A β levels were significantly increased by 5–8-fold that in astrocytes incubated without LPL. Next,

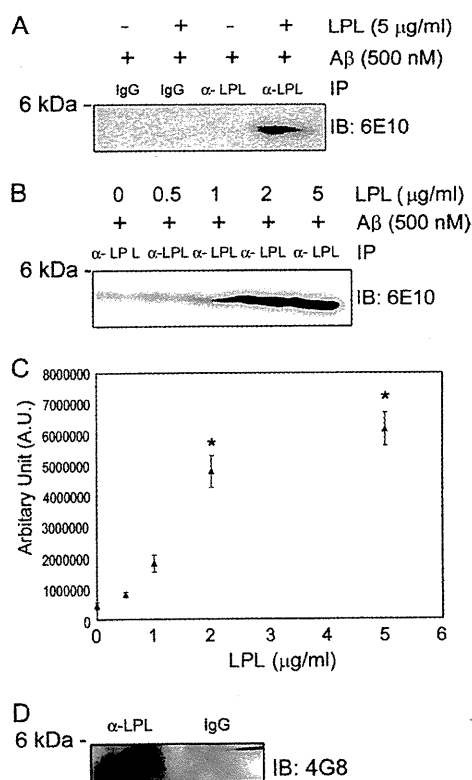


FIGURE 1. LPL binds to A β *in vitro*. A, LPL (5 μ g/ml) and A β (500 nM) were incubated in DMEM at 37 °C for 3 h. Protein complexes formed were immunoprecipitated with an anti-LPL antibody (α -LPL), and the immunoprecipitates (IP) were analyzed by Western blotting using 6E10, an anti-A β antibody. These data are representative of three independent experiments. B, LPL at various concentrations of 0, 0.5, 1, 2, and 5 μ g/ml and A β at 500 nM were incubated in DMEM at 37 °C for 3 h. Protein complexes formed were immunoprecipitated with an α -LPL, and the immunoprecipitates were subjected to Western blotting using 6E10. C, quantification of A β immunoprecipitated with α -LPL. The data presented are the means \pm S.D. of three independent experiments. *, *p* < 0.001 versus samples without LPL treatment. D, the mouse cerebrum was homogenized by sonication in 4 volumes of PBS containing a protease inhibitor mixture and centrifuged at 1000 \times *g* for 10 min at 4 °C. The supernatants were harvested. LPL-A β complexes in the supernatant were immunoprecipitated with an α -LPL, and the A β in the immunoprecipitates was detected by Western blotting using 4G8, an anti-A β antibody. IB, immunoblot.

we determined the time-dependent effect of LPL-mediated A β uptake into astrocytes. Astrocyte cultures were incubated with A β (500 nM) and LPL (2 μ g/ml) at 37 °C for various hours, and the A β level in the cell lysate was determined. The level of A β in the cell lysate increased in a time-dependent manner (Fig. 2E). The A β levels in the astrocytes incubated for 3 and 5 h were significantly higher by 9–14-fold of that in astrocytes incubated without LPL (Fig. 2F). These concentrations of LPL are comparable with the concentrations with which LPL could act as “bridging molecules” (2, 20). There were no significant differences among the values for cultures without LPL (one-way ANOVA, *p* = 0.1386). No change in cellular morphology or cell number in astrocyte cultures was observed during the incubation (data not shown). To examine the involvement of LPL expressed by astrocytes, we carried out experiments using the gene silencing technique for LPL. The transient knockdown of LPL expression was achieved by the transfection of siRNA specific for LPL. After transfection,

LPL Promotes A β Cellular Uptake

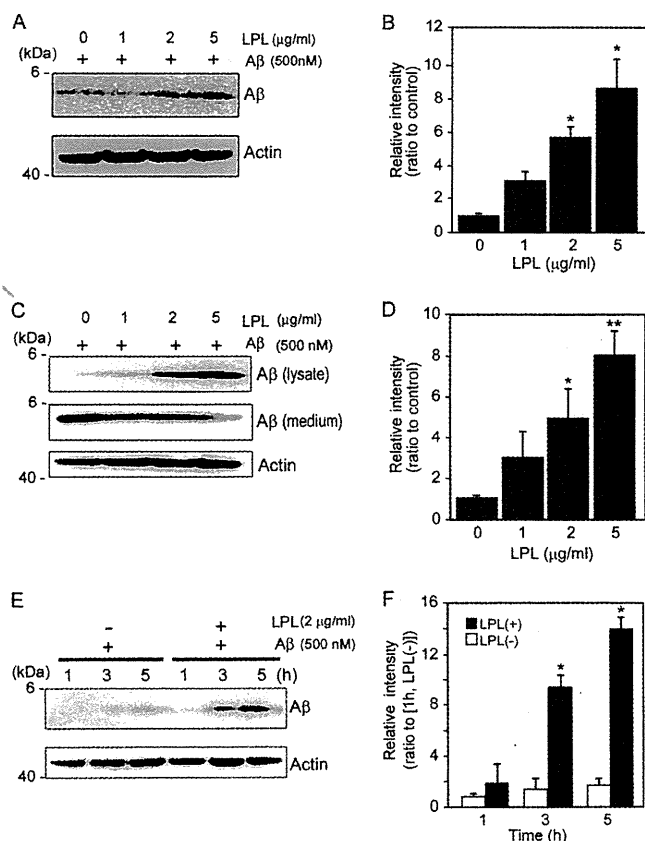


FIGURE 2. LPL augments cell-surface association and cellular uptake of A β in astrocytes. *A*, mouse primary astrocytes were incubated with LPL (0–5 μ g/ml) and A β (500 nM) at 4 °C for 3 h. The astrocytes were washed in cold PBS three times, and the cells were harvested using a scraper. The level of A β on the cell surface was determined by Western blotting in a detergent extract of whole cells. *B*, quantification of cell-surface-associated A β . The data are the means \pm S.D. of three independent experiments. *, $p < 0.001$ versus LPL at 0 μ g/ml. *C* and *D*, astrocytes were incubated with A β (500 nM) and LPL (0, 1, 2, and 5 μ g/ml) at 37 °C for 3 h. The cultured cells were then washed thoroughly in PBS for three times, and the cells were collected. The level of A β in the whole cell lysate (*lysate*), and the conditioned medium of cultured cells (*medium*) were determined by Western blotting using 6E10 antibody. The level of actin demonstrated by Western blotting using an anti- β -actin antibody was used as the loading control. These data are representative of at least three independent experiments. *D*, quantification of cellular A β is shown. The data presented are the means \pm S.D. of three independent experiments. *, $p < 0.05$; **, $p < 0.01$ versus LPL at 0 μ g/ml. *E* and *F*, astrocytes were incubated with A β (500 nM) and LPL (2 μ g/ml) at 37 °C for 0, 3, and 5 h. The cultured cells were then washed thoroughly in PBS three times, and the cells were collected. The amount of A β in the whole cell lysate was determined by Western blotting using 6E10 antibody. The level of actin demonstrated by Western blotting using the anti- β -actin antibody was used as the loading control. These data are representative of at least three independent experiments. *F*, quantification of cellular A β is shown. The data are the means \pm S.D. of three independent experiments. *, $p < 0.001$ versus LPL (+) at 1 h.

cells were treated with A β 42 (1 μ M) and then incubated at 4 °C for 3 h. As shown in Fig. 3, the cellular binding of A β 42 to astrocytes was significantly decreased by LPL protein knockdown.

Degradation of Internalized A β in a Lysosomal Pathway in Astrocytes—Next, we examined the degradation of internalized A β . Mouse primary astrocytes were incubated with soluble A β 42 and LPL at 37 °C for 5 h, washed in DMEM three times, and cultured at 37 °C for additional time (0, 3, 5, 12,

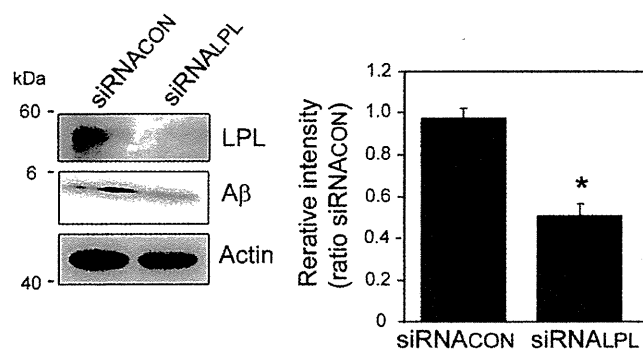


FIGURE 3. Effect of LPL knockdown on cell-surface association of A β in cultured astrocytes. Astrocytes were transfected with 10 nM siRNA specific for LPL (*siRNA LPL*) and control siRNA (*siRNA CON*). Forty-eight hours after transfection, cells were treated with A β 42 (1 μ M) at 4 °C for 3 h. The cells were washed in cold PBS three times, and the cells were harvested using a scraper. The level of A β 42 on the cell surface was determined by Western blotting in a detergent extract of whole cells. The graph shows the levels of cell-surface-associated A β . The data are the means \pm S.D. of three independent experiments. *, $p < 0.001$ versus control siRNA by unpaired Student's *t* test.

and 24 h). Cells were then harvested, and the A β level in the cell lysate was analyzed by Western blotting. The strong signal representing internalized A β during the initial incubation for 5 h was detected in the cell lysate at the point of 0 min after washing (Fig. 4*A*). Three to five hours after washing, the level of A β remaining in the cell lysate partially disappeared (Fig. 4*A*). Twelve and twenty-four hours after washing, the internalized A β completely disappeared, indicating that the internalized A β was degraded in astrocytes in a time-dependent manner (Fig. 4*A*). To gain insight into the degradation pathway of the internalized A β , we investigated the localization of A β by immunocytochemical analysis. Mouse primary astrocytes were plated on poly-L-lysine-coated coverglasses and incubated with A β 42 (500 nM) and LPL (2 μ g/ml) at 37 °C for 5 h. In some experiments, cells were washed in DMEM three times and further incubated in serum-free DMEM for 3 h. Cells were then permeabilized and stained with an anti-A β antibody, 6E10, and an anti-LAMP2 antibody, whose staining signal is considered as a marker of late endosomes/lysosomes (21). We found that some portions of anti-A β antibody-positive signals were co-localized with staining signals reactive to the anti-LAMP2 antibody, showing that the internalized A β was trafficked into late endosomal/lysosomal compartments (Fig. 4*B*). To confirm the involvement of a lysosomal pathway in the degradation of LPL-mediated internalized A β , we determined the effect of chloroquine on the localization of A β internalized in an LPL-mediated manner. Chloroquine is a weak base and is taken up by cells, which results in the neutralization of acidic organelles such as lysosomes and impairment of their functions (22, 23). Chloroquine treatment at concentrations of 25 and 50 μ g/ml prevented the degradation of internalized A β 12 h after washing out (Fig. 4*C*). We also tested inhibitors of neprilysin, an insulin-degrading enzyme, and cathepsin B, all of which are known to degrade A β . These inhibitors failed to suppress the degradation of internalized A β in astrocytes (data not shown). Thus, A β internalized in an LPL-mediated manner was degraded in a lysosomal pathway in astrocytes.

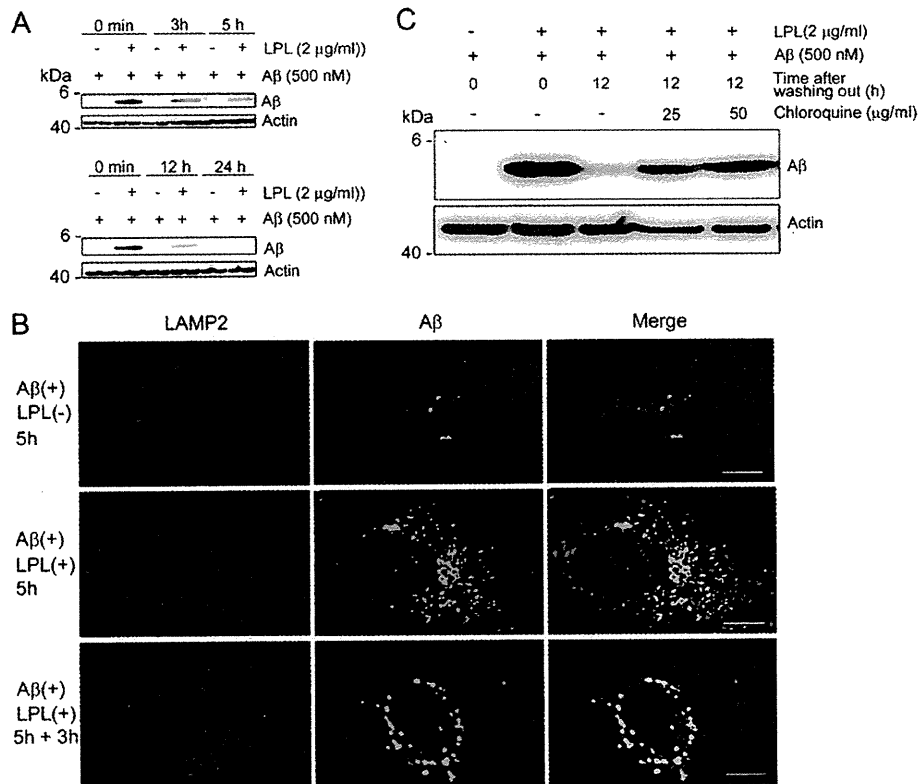


FIGURE 4. A β is trafficked to late endosomal/lysosomal compartments and degraded after the LPL-mediated uptake. *A*, mouse primary astrocytes were incubated with LPL (2 μ g/ml) and A β (500 nM) at 37 °C for 5 h. Cells were washed in DMEM three times and then incubated in DMEM at 37 °C for 0, 3, 5, 12, and 24 h. The amount of A β remaining in the cells was determined by Western blotting using the anti-A β antibody, 6E10, in a detergent extract of whole cells. *B*, astrocytes were plated on poly-L-lysine-coated coverglasses and incubated with LPL (2 μ g/ml) and A β (250 nM) at 37 °C for 5 h. Then, cells were permeabilized and double stained with an anti-LAMP2 antibody and 2C8. Bound antibodies were visualized with Cy3-conjugated (red) and FITC-conjugated (green) secondary antibodies for the anti-LAMP2 antibody and 6E10, respectively. Astrocytes incubated without A β did not show any anti-A β antibody-positive signals (not shown). Scale bar, 10 μ m. *C*, astrocytes were incubated with LPL (2 μ g/ml) and A β (500 nM) at 37 °C for 5 h. Cells were then washed in DMEM and cultured with or without chloroquine in DMEM at 37 °C for an additional 12 h. The level of A β in the detergent extract of whole cells was determined by Western blotting with 6E10. These are representative data of at least three independent experiments.

LPL Promotes Cellular Uptake of A β in a Heparan Sulfate- and Chondroitin Sulfate-dependent Manner—LPL has a high affinity with heparan sulfate (HS) and chondroitin sulfate (CS) (5, 24, 25). Therefore, we next investigated whether HS and CS are involved in the LPL-mediated cellular binding and cellular uptake of A β in astrocytes. Mouse primary astrocytes were pretreated with a mixture of heparinase II and heparinase III and/or chondroitinase ABC for 24 h at 37 °C, followed by incubation with A β 42 and LPL at 4 °C for 3 h. There were no significant differences among the values in the absence of LPL (one-way ANOVA; $p = 0.0929$ for cell-surface-associated A β , $p = 0.4350$ for cellular A β). Pretreatment with heparinases or chondroitinase ABC partially decreased the level of LPL-mediated cellular binding of A β in astrocytes to 40 or 50% of that observed in the nontreated control, respectively (Fig. 5A). Interestingly, pretreatment with both heparinases and chondroitinase ABC decreased the level of LPL-mediated binding of A β to astrocytes to 20% of that observed in nontreated control (Fig. 5A). Next, we determined the effect of HS and/or CS on the LPL-mediated cellular uptake of A β . In conjunction with the effect of LPL on A β binding, heparinases and chondroitinase ABC decreased the level of LPL-mediated cellular uptake of A β in astrocytes to 30 and 50% of

that observed in the nontreated control incubated with LPL, respectively (Fig. 5B). Pretreatment with both heparinases and chondroitinase ABC did not show an additive effect on the attenuation of LPL-promoted A β uptake (Fig. 5B). These findings indicate that HS and CS expressed in astrocytes are involved in the LPL-mediated association of A β with astrocytes and A β cellular uptake.

To further confirm the involvement of HS and CS in LPL-mediated A β uptake, we incubated astrocytes with various glycosaminoglycans. Heparin, which is a structural analog of HS, substantially suppressed the effect of LPL on A β uptake at a concentration of 3 μ g/ml (Fig. 5C). The suppressive effect of heparin on LPL-mediated A β uptake was also observed in the presence of de-N-sulfated heparin, whereas either de-2-O-sulfated heparin or de-6-O-sulfated heparin had no effect on LPL-mediated A β uptake (Fig. 5C). None of these heparins interfered with the interaction between LPL and A β (Fig. 5D). In addition, 4-O-, 6-O-disulfated chondroitin sulfate (3 μ g/ml) completely suppressed the promotive effect of LPL on A β uptake (Fig. 5E). 4-O-Sulfated chondroitin sulfate and 6-O-sulfated chondroitin sulfate moderately attenuated the function of LPL, whereas chondroitin (a nonsulfated form of chondroitin sulfate) and 2-O-, 6-O-disulfated chondroitin

LPL Promotes A β Cellular Uptake

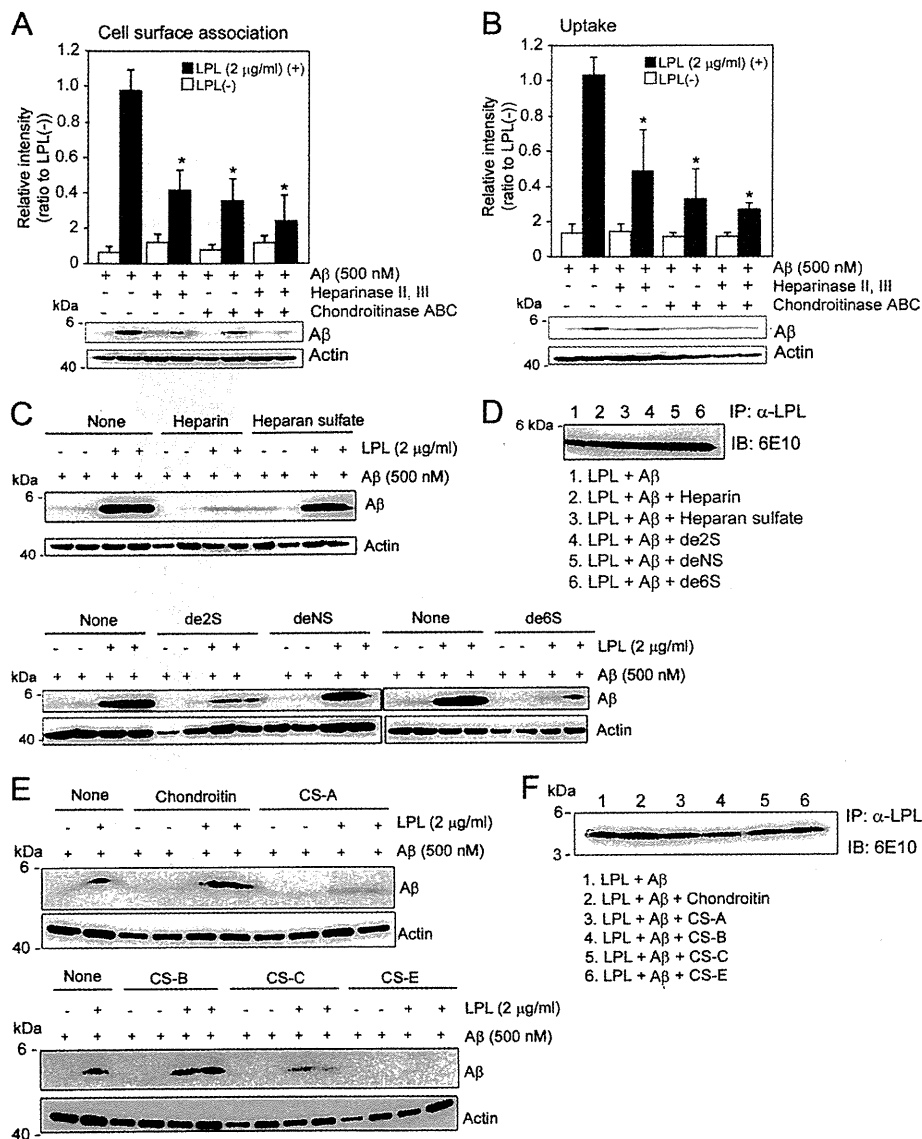


FIGURE 5. LPL-mediated cellular binding and uptake of A β depends on heparan sulfate and chondroitin sulfate in astrocytes. *A* and *B*, astrocytes from wild-type mice were pretreated with a mixture of heparinase II (0.03 μ g/ml) and heparinase III (0.03 μ g/ml), and/or chondroitinase ABC (0.03 μ g/ml) at 37 °C for 24 h. After washing in DMEM three times, cells were incubated with LPL (2 μ g/ml) and A β (500 nM) at 4 °C for 3 h (for cell surface association) (*A*) or 37 °C for 3 h (for uptake) (*B*). The level of A β in the detergent extract of whole cells was determined by Western blotting using 6E10. The quantitative assessment of cell-surface-associated A β (*A*) and cellular A β (*B*) in the present (closed bars) or absence (open bars) of LPL are shown. The data presented are the means \pm S.D. of three independent experiments. **p* < 0.001 versus levels of LPL (-). (*C*) Mouse primary astrocytes were incubated with A β (500 nM) or LPL (2 μ g/ml) and A β (500 nM) in the presence or absence of heparin or chemically modified heparins at a concentration of 3 μ g/ml at 37 °C for 3 h. The level of A β in the detergent extract of whole cells was determined using 6E10. (*D*) LPL (2 μ g/ml) and A β (500 nM) were incubated in DMEM at 37 °C for 3 h in the presence or absence of heparin, heparan sulfate, or chemically modified heparins at a concentration of 3 μ g/ml. Protein complexes in DMEM were immunoprecipitated (IP) with an anti-LPL antibody (α -LPL) and the A β recovered in the immunoprecipitates was analyzed by Western blotting using 6E10. These data are representative of at least three independent experiments. *de2S*, 2-*O*-desulfated heparin; *de6S*, 6-*O*-desulfated heparin; *deNS*, *N*-desulfated heparin. *E*, astrocytes were incubated with LPL (2 μ g/ml) and A β (500 nM) in the presence or absence of chondroitin sulfates (chondroitin, chondroitin 4-sulfate (CS-A), 2-*O*-, 6-*O*-disulfated chondroitin sulfate (CS-B), 6-*O*-sulfated chondroitin sulfate (CS-C), and chondroitin 4,6-disulfate (CS-E)) at a concentration of 3 μ g/ml at 37 °C for 5 h. The level of A β in a detergent extract of whole cells was determined by Western blotting using 6E10. *F*, LPL (2 μ g/ml) and A β (500 nM) were incubated in DMEM at 37 °C for 3 h in the presence or absence of chondroitin sulfates at a concentration of 3 μ g/ml. Protein complexes were immunoprecipitated with the anti-LPL antibody (α -LPL), and the A β recovered in the immunoprecipitates was analyzed by Western blotting using 6E10. The data are representative of at least three independent experiments. *IB*, immunoblot.

sulfate (also known as dermatan sulfate) did not (Fig. 5*E*). None of these CS interfered with the interaction between LPL and A β *in vitro* (Fig. 5*F*).

ApoE Is Dispensable for LPL-mediated Cellular Uptake of A β in Astrocytes—Because ApoE is reported to be involved in the metabolism of A β , including its aggregation and clearance

(26), we analyzed the effects of ApoE on the LPL-mediated cellular uptake of A β in astrocytes. We collected culture media of primary astrocytes prepared from ApoE-KO mice and C57BL/6 (WT) mice. The astrocyte cultures prepared from wild-type mouse cortices were incubated in conditioned media in the presence of A β 42 and LPL. As shown in Fig. 6*A*, A β

LPL Promotes A β Cellular Uptake

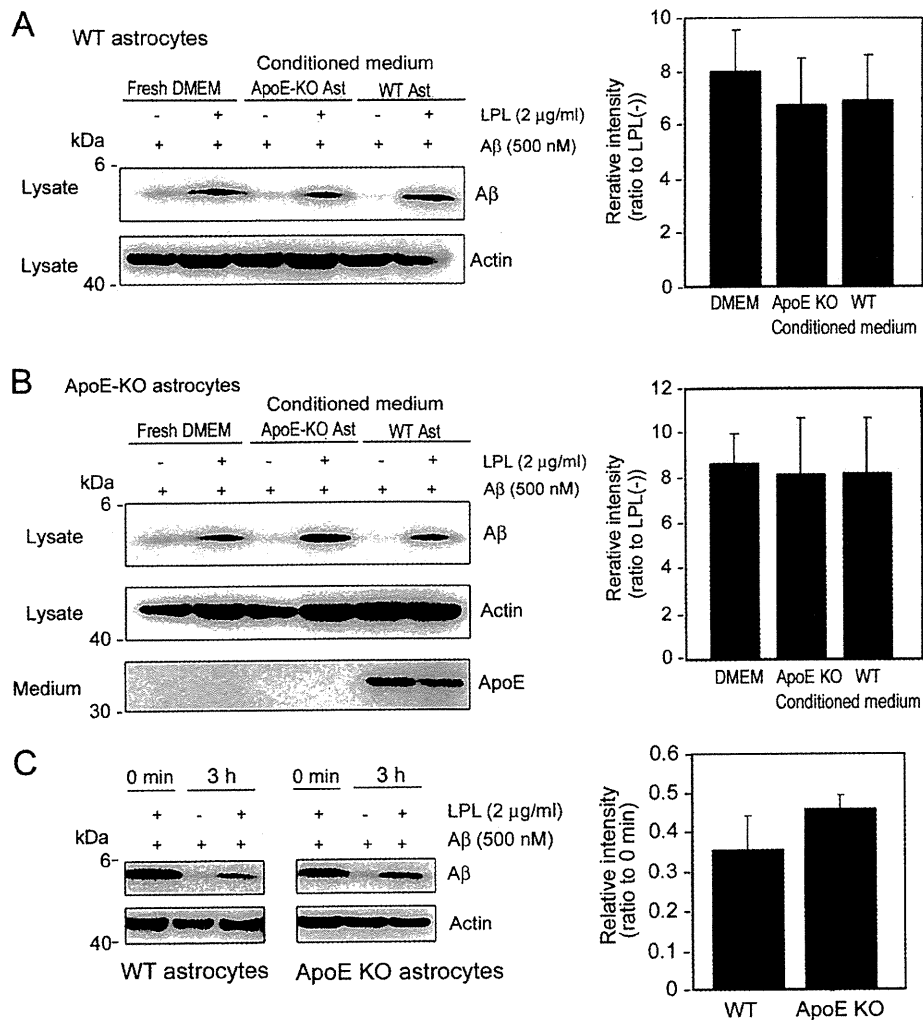


FIGURE 6. ApoE is dispensable for the LPL-mediated cellular uptake of A β in astrocytes. The astrocyte cultures prepared from WT or ApoE knock-out (KO) mice were incubated in fresh serum-free DMEM for 3 days at 37 °C. The conditioned media of these cultures were then collected. The astrocytes prepared from WT (A) or ApoE-KO (B) mouse brains were incubated in the conditioned medium of ApoE-KO astrocyte cultures or conditioned medium of WT astrocyte cultures, and LPL (2 μ g/ml) and A β (500 nM) were added into each culture; the cultures were then maintained for another 5 h at 37 °C. After the incubation, the cultures were harvested, and the amount of cellular A β in a detergent extract of whole cells (*lysate*) was determined by Western blotting using 6E10. The amount of ApoE in the conditioned medium of cultured cells (*medium*) was determined by Western blotting using an anti-ApoE antibody, AB947. These data are representative of at least three independent experiments. The graphs show the cellular A β levels. The data are the means \pm S.D. of three independent experiments. *CM*, conditioned medium; *Ast*, astrocytes. C, mouse primary astrocytes from WT and ApoE-KO mice were incubated with soluble A β 42 in the presence or absence of LPL at 37 °C for 5 h, washed in DMEM three times, and further incubated at 37 °C for 3 h. Cells were then harvested, and the A β levels in the lysate was analyzed by Western blotting. The graph shows the cellular A β levels. The data are the means \pm S.D. of three independent experiments.

uptake was promoted by LPL in astrocytes prepared from WT mice incubated in a fresh medium, the conditioned medium from ApoE-KO astrocytes, and the conditioned medium from WT astrocytes. There were no significant differences between these three groups (one-way ANOVA; $p = 0.6419$). This is also the case for ApoE-KO astrocytes (one-way ANOVA; $p = 0.9467$) (Fig. 6B). These findings indicate that ApoE is dispensable for the LPL-promoted cellular uptake of A β in astrocytes. We also examined the effects of ApoE on the degradation of internalized A β . Primary astrocytes from WT and ApoE-KO mice were incubated with soluble A β 42 and LPL at 37 °C for 5 h, washed in DMEM three times, and further incubated at 37 °C for 3 h. Cells were then harvested, and the A β level in the cell lysate was analyzed by Western blotting. As

shown in Fig. 6C, there were no significant differences between the levels of A β remaining in the lysate of WT astrocytes and ApoE-KO astrocytes ($p = 0.1031$).

DISCUSSION

Previous studies have shown that the mRNA expression of the LPL gene and the enzymatically active LPL are found in the brain in several mammalian species (6, 7, 27). However, considering that the main fraction of lipoproteins in the brain is HDL, which contains negligible or no triacylglycerols, and that the brain lacks an essential cofactor, apoCII, it is conceivable that LPL has a different function in the brain from that in the systemic circulation serving as an enzyme with the cofactor apoCII to catalyze the hydrolysis of triacylglycerols (28). In

LPL Promotes A β Cellular Uptake

the present study, we found a novel function of LPL serving as an A β binding molecule; that is, exogenous LPL binds to A β and promotes cellular binding and uptake of A β in astrocytes. The internalized A β was degraded within 12 h, mainly in a lysosomal pathway. Furthermore, we have demonstrated that HS and CS glycosaminoglycans are involved in the promotion of the LPL-mediated cellular uptake of A β in astrocytes.

Astrocytes are a major glial cell type in the CNS and play a crucial role in neuronal development, maintenance of synapse functions, and CNS repair after injury. Additionally, astrocytes have phagocytic and proteolytic activities (29, 30) and ingest A β (15, 31, 32). Our results indicate that LPL strongly enhances cellular uptake of A β , leading to increased degradation of A β in astrocytes. Previous studies have shown that SNPs in the coding region of the LPL gene are associated with AD development (33) and the severity of AD pathophysiological features (12), with the molecular mechanisms underlying this association remaining unknown. It may be possible that altered function of LPL shown in this study would result in impaired A β clearance and subsequent accumulation of A β , accelerating AD development. Because the accumulation of A β in the extracellular space is considered to trigger A β aggregation and deposition, the function of LPL to enhance A β binding, uptake, and degradation in astrocytes may decrease A β levels in the brain. However, because LPL is known to regulate the uptake and transport of vitamin E to the brain, of which deficiency results in increased A β accumulation and presynaptic defects accompanied by impaired learning and memory function *in vivo* (34, 35), there may be other possibilities as well, that the altered LPL function regulating vitamin E transport may enhance A β accumulation and impair synaptic function.

It has been suggested that lysosomal dysfunction plays a major role in A β accumulation, thereby causing neuronal cell death (36, 37) and that chloroquine, which disrupts lysosomal pH balance, enhances A β accumulation in a microglial cell line (38). Our results show that almost all of the internalized A β was localized in lysosomes and degraded in a time-dependent manner, and this degradation was markedly inhibited by the treatment with chloroquine, suggesting that A β was degraded mainly in a lysosomal pathway. These findings suggest that lysosomal pathways play a critical role in the degradation of A β that is internalized via a novel pathway as LPL-A β complexes by astrocytes.

It has been shown that LPL associates with lipoproteins and the formed LPL-bound lipoprotein complexes bind to cell-surface HS proteoglycans and CS proteoglycans (1, 5, 39), promoting the cellular uptake of lipoproteins by acting as a bridging molecule (2, 40). HS proteoglycans and CS proteoglycans are present in astrocytes (41–43). We found that pretreatment of astrocytes with a mixture of heparinases or chondroitinase ABC partially attenuated the LPL-mediated A β uptake, and cotreatment with heparinases and chondroitinase ABC completely suppressed the LPL-mediated cellular uptake of A β (Fig. 4), indicating that the LPL-mediated cellular uptake of A β is mediated via HS proteoglycans and CS proteoglycans. Interestingly, heparin, a highly sulfated form of HS, and 4-*O*-, 6-*O*-disulfated chondroitin sulfate, a highly

sulfated CS, selectively suppressed the promotion of A β uptake in astrocytes. These findings suggest that LPL could act as a bridging molecule between not only cell-surface GAGs and lipoproteins but also cell-surface GAGs and A β and facilitate the cellular uptake of A β in astrocytes and that certain domains modified by multiple sulfate groups are necessary for LPL to function in astrocytes.

ApoE is one of the major apolipoproteins in the brain and plays a key role in lipid transport in the brain. ApoE affects the aggregation of A β *in vitro* (26). PDAPP and Tg2576 transgenic mice exhibit extensive cerebral A β deposition. When these transgenic mice lack the murine *apoE* gene, a significant decrease in amyloid plaque formation was observed (44, 45). Furthermore, two *in vitro* studies have demonstrated that ApoE can facilitate the cellular degradation of A β (16, 31). These lines of evidence suggest that ApoE affects A β metabolism. Thus, we examined whether ApoE could be involved in the LPL-mediated cellular uptake of A β . LPL promoted the cellular uptake of A β in wild-type and ApoE-deficient astrocytes in culture. The presence or absence of ApoE in the conditioned medium of astrocytes did not alter the levels of A β internalized in an LPL-mediated manner. These results suggest that ApoE is not required for the LPL-mediated cellular uptake of A β in astrocytes.

In this study, we demonstrated a novel LPL function; that is, LPL binds to A β and enhances the cellular uptake of A β in a sulfated glycosaminoglycan-dependent manner, and the internalized A β is degraded in a lysosomal pathway. Although further studies will be needed to confirm the role of LPL in the clearance of A β *in vivo*, our findings provide a new insight into the molecular pathogenesis of AD and a potential strategy for AD therapy.

REFERENCES

- Williams, K. J., Fless, G. M., Petrie, K. A., Snyder, M. L., Brocia, R. W., and Swenson, T. L. (1992) *J. Biol. Chem.* **267**, 13284–13292
- Mulder, M., Lombardi, P., Jansen, H., van Berkel, T. J., Frants, R. R., and Havekes, L. M. (1993) *J. Biol. Chem.* **268**, 9369–9375
- Kreuger, J., Spillmann, D., Li, J. P., and Lindahl, U. (2006) *J. Cell Biol.* **174**, 323–327
- Edwards, I. J., Goldberg, I. J., Parks, J. S., Xu, H., and Wagner, W. D. (1993) *J. Lipid Res.* **34**, 1155–1163
- Edwards, I. J., Xu, H., Obunike, J. C., Goldberg, I. J., and Wagner, W. D. (1995) *Arterioscler. Thromb. Vasc. Biol.* **15**, 400–409
- Goldberg, I. J., Soprano, D. R., Wyatt, M. L., Vanni, T. M., Kirchgessner, T. G., and Schotz, M. C. (1989) *J. Lipid Res.* **30**, 1569–1577
- Yacoub, L. K., Vanni, T. M., and Goldberg, I. J. (1990) *J. Lipid Res.* **31**, 1845–1852
- Eckel, R. H., and Robbins, R. J. (1984) *Proc. Natl. Acad. Sci. U.S.A.* **81**, 7604–7607
- Havel, R. J., Fielding, C. J., Olivecrona, T., Shore, V. G., Fielding, P. E., and Egelrud, T. (1973) *Biochemistry* **12**, 1828–1833
- Zannis, V. I., Cole, F. S., Jackson, C. L., Kurnit, D. M., and Karathanasis, S. K. (1985) *Biochemistry* **24**, 4450–4455
- Rebeck, G. W., Harr, S. D., Strickland, D. K., and Hyman, B. T. (1995) *Ann. Neurol.* **37**, 211–217
- Blain, J. F., Aumont, N., Théroux, L., Dea, D., and Poirier, J. (2006) *Eur. J. Neurosci.* **24**, 1245–1251
- Iwatsubo, T., Odaka, A., Suzuki, N., Mizusawa, H., Nukina, N., and Ihara, Y. (1994) *Neuron* **13**, 45–53
- Tanzi, R. E., Moir, R. D., and Wagner, S. L. (2004) *Neuron* **43**, 605–608
- Wyss-Coray, T., Loike, J. D., Brionne, T. C., Lu, E., Anankov, R., Yan, F.,

- Silverstein, S. C., and Husemann, J. (2003) *Nat. Med.* **9**, 453–457
16. Jiang, Q., Lee, C. Y., Mandrekar, S., Wilkinson, B., Cramer, P., Zelcer, N., Mann, K., Lamb, B., Willson, T. M., Collins, J. L., Richardson, J. C., Smith, J. D., Comery, T. A., Riddell, D., Holtzman, D. M., Tontonoz, P., and Landreth, G. E. (2008) *Neuron* **58**, 681–693
 17. Majumdar, A., Cruz, D., Asamoah, N., Buxbaum, A., Sohar, I., Lobel, P., and Maxfield, F. R. (2007) *Mol. Biol. Cell* **18**, 1490–1496
 18. Mandrekar, S., Jiang, Q., Lee, C. Y., Koenigsnecht-Talboo, J., Holtzman, D. M., and Landreth, G. E. (2009) *J. Neurosci.* **29**, 4252–4262
 19. Michikawa, M., Gong, J. S., Fan, Q. W., Sawamura, N., and Yanagisawa, K. (2001) *J. Neurosci.* **21**, 7226–7235
 20. Fernández-Borja, M., Bellido, D., Vilella, E., Olivecrona, G., and Vilaró, S. (1996) *J. Lipid Res.* **37**, 464–481
 21. Fukuda, M. (1991) *J. Biol. Chem.* **266**, 21327–21330
 22. de Duve, C., de Barse, T., Poole, B., Trouet, A., Tulkens, P., and Van Hoof, F. (1974) *Biochem. Pharmacol.* **23**, 2495–2531
 23. Poole, B., and Ohkuma, S. (1981) *J. Cell Biol.* **90**, 665–669
 24. Bengtsson, G., Olivecrona, T., Höök, M., Riesenfeld, J., and Lindahl, U. (1980) *Biochem. J.* **189**, 625–633
 25. Pillarisetti, S., Paka, L., Sasaki, A., Vanni-Reyes, T., Yin, B., Parthasarathy, N., Wagner, W. D., and Goldberg, I. J. (1997) *J. Biol. Chem.* **272**, 15753–15759
 26. Kim, J., Basak, J. M., and Holtzman, D. M. (2009) *Neuron* **63**, 287–303
 27. Brecher, P., and Kuan, H. T. (1979) *J. Lipid Res.* **20**, 464–471
 28. Koch, S., Donarski, N., Goetze, K., Kreckel, M., Stuerenburg, H. J., Buhmann, C., and Beisiegel, U. (2001) *J. Lipid Res.* **42**, 1143–1151
 29. al-Ali, S. Y., and al-Hussain, S. M. (1996) *J. Anat.* **188**, 257–262
 30. Hatten, M. E., Liem, R. K., Shelanski, M. L., and Mason, C. A. (1991) *Glia* **4**, 233–243
 31. Koistinaho, M., Lin, S., Wu, X., Esterman, M., Koger, D., Hanson, J., Higgs, R., Liu, F., Malkani, S., Bales, K. R., and Paul, S. M. (2004) *Nat. Med.* **10**, 719–726
 32. Matsunaga, W., Shirokawa, T., and Isobe, K. (2003) *Neurosci. Lett.* **342**, 129–131
 33. Baum, L., Chen, L., Masliah, E., Chan, Y. S., Ng, H. K., and Pang, C. P. (1999) *Am. J. Med. Genet.* **88**, 136–139
 34. Xian, X., Liu, T., Yu, J., Wang, Y., Miao, Y., Zhang, J., Yu, Y., Ross, C., Karasinska, J. M., Hayden, M. R., Liu, G., and Chui, D. (2009) *J. Neurosci.* **29**, 4681–4685
 35. Nishida, Y., Ito, S., Ohtsuki, S., Yamamoto, N., Takahashi, T., Iwata, N., Jishage, K., Yamada, H., Sasaguri, H., Yokota, S., Piao, W., Tomimitsu, H., Saido, T. C., Yanagisawa, K., Terasaki, T., Mizusawa, H., and Yokota, T. (2009) *J. Biol. Chem.* **284**, 33400–33408
 36. Bahr, B. A., and Bendiske, J. (2002) *J. Neurochem.* **83**, 481–489
 37. Nixon, R. A., Cataldo, A. M., and Mathews, P. M. (2000) *Neurochem. Res.* **25**, 1161–1172
 38. Chu, T., Tran, T., Yang, F., Beech, W., Cole, G. M., and Frautschy, S. A. (1998) *FEBS Lett.* **436**, 439–444
 39. Eisenberg, S., Sehayek, E., Olivecrona, T., and Vlodavsky, I. (1992) *J. Clin. Invest.* **90**, 2013–2021
 40. Auerbach, B. J., Bisgaier, C. L., Wölle, J., and Saxena, U. (1996) *J. Biol. Chem.* **271**, 1329–1335
 41. Hsueh, Y. P., and Sheng, M. (1999) *J. Neurosci.* **19**, 7415–7425
 42. Laabs, T. L., Wang, H., Katagiri, Y., McCann, T., Fawcett, J. W., and Geller, H. M. (2007) *J. Neurosci.* **27**, 14494–14501
 43. Tsuchida, K., Shioi, J., Yamada, S., Boghosian, G., Wu, A., Cai, H., Sugahara, K., and Robakis, N. K. (2001) *J. Biol. Chem.* **276**, 37155–37160
 44. Bales, K. R., Verina, T., Dodel, R. C., Du, Y., Altstiel, L., Bender, M., Hyslop, P., Johnstone, E. M., Little, S. P., Cummins, D. J., Piccardo, P., Ghetti, B., and Paul, S. M. (1997) *Nat. Genet.* **17**, 263–264
 45. Holtzman, D. M., Bales, K. R., Wu, S., Bhat, P., Parsadanian, M., Fagan, A. M., Chang, L. K., Sun, Y., and Paul, S. M. (1999) *J. Clin. Invest.* **103**, R15–R21

Apolipoprotein E Regulates the Integrity of Tight Junctions in an Isoform-dependent Manner in an *in Vitro* Blood-Brain Barrier Model*

Received for publication, January 27, 2011, and in revised form, March 28, 2011. Published, JBC Papers in Press, April 6, 2011, DOI 10.1074/jbc.M111.225532

Kazuchika Nishitsuji[‡], Takashi Hosono[‡], Toshiyuki Nakamura[‡], Guojun Bu[§], and Makoto Michikawa^{‡1}

From the [‡]Department of Alzheimer's Disease Research, National Institute for Longevity Sciences, National Center for Geriatrics and Gerontology, Obu, Aichi 474-8522, Japan and the [§]Department of Neuroscience, Mayo Clinic, Jacksonville, Florida 32224

Apolipoprotein E (apoE) is a major apolipoprotein in the brain. The $\epsilon 4$ allele of apoE is a major risk factor for Alzheimer disease, and apoE deficiency in mice leads to blood-brain barrier (BBB) leakage. However, the effect of apoE isoforms on BBB properties are as yet unknown. Here, using an *in vitro* BBB model consisting of brain endothelial cells and pericytes prepared from wild-type (WT) mice, and primary astrocytes prepared from human apoE3- and apoE4-knock-in mice, we show that the barrier function of tight junctions (TJs) was impaired when the BBB was reconstituted with primary astrocytes from apoE4-knock-in mice (apoE4-BBB model). The phosphorylation of occludin at Thr residues and the activation of protein kinase C (PKC) η in mBECs were attenuated in the apoE4-BBB model compared with those in the apoE3-BBB model. The differential effects of apoE isoforms on the activation of PKC η , the phosphorylation of occludin at Thr residues, and TJ integrity were abolished following the treatment with an anti-low density lipoprotein receptor-related protein 1 (LRP1) antibody or a LRP1 antagonist receptor-associated protein. Consistent with the results of *in vitro* studies, BBB permeability was higher in apoE4-knock-in mice than in apoE3-knock-in mice. Our studies provide evidence that TJ integrity in BBB is regulated by apoE in an isoform-dependent manner.

Apolipoprotein E (apoE)² is a polymorphic glycoprotein with a molecular mass of 34 kDa. Its three isoforms, apoE2, apoE3, and apoE4, are all products of the same gene, which exists as three alleles ($\epsilon 2$, $\epsilon 3$, and $\epsilon 4$) at a single locus (1). Among these three isoforms, apoE4 is a major risk factor for Alzheimer dis-

ease (AD) (2, 3). ApoE is expressed in several organs, with the liver showing the highest expression level, followed by the brain. In the brain, apoE is a major apolipoprotein and plays a major role in the transportation of lipids as a lipid acceptor (1). ApoE-containing lipoprotein particles are mainly produced by astrocytes and deliver cholesterol and other essential lipids to neurons through low density lipoprotein (LDL) receptor family members (4–6). A number of studies revealed that astrocytes are involved in the control of endothelium blood-brain barrier (BBB) properties (7, 8) and that apoE deficiency leads to BBB leakage (9–11).

BBB is formed by brain endothelial cells and is essential for the protection of the central nervous system from harmful blood molecules and cells (12). Brain endothelial cells form tight junctions (TJs), which are the fundamental characteristics of BBB (13, 14). The assembly of TJs requires at least three types of transmembrane protein, namely, occludin, claudin, and junctional adhesion molecule (15). Protein kinases are localized at TJs or interact directly with TJ proteins (16–18). Among protein kinases, PKC η has been shown to regulate the phosphorylation of occludin at its Thr residues and play a crucial role in the assembly and/or maintenance of TJs (19). Cells surrounding brain capillaries, such as astrocytes and pericytes, contribute to the formation of a functional BBB (20). Interaction between astrocytes and brain endothelial cells is likely important for TJ formation and maintenance.

Recently, an *in vitro* BBB model in triple co-culture consisting of brain endothelial cells, pericytes, and astrocytes has been established (21). To determine whether apoE-containing particles secreted from astrocytes regulate TJ integrity in BBB, we investigated the effects of apoE isoforms on TJ integrity, using a triple co-culture model consisting of primary brain endothelial cells and pericytes, both of which were prepared from wild-type (WT) mice, and primary astrocytes prepared from human apoE3- or apoE4-knock-in mice, WT mice, or apoE-knock-out (apoE-KO) mice. Here, we provide evidence that apoE regulates PKC η activity and the phosphorylation of occludin at its Thr residues in an isoform-dependent manner, which regulate TJ functions. The expression of occludin was not affected by either isoform. Transendothelial electric resistance (TEER), an important parameter of TJ integrity in a culture model, was lower in the model using astrocytes from apoE4-knock-in mice (apoE4-BBB model) than in the model using astrocytes from apoE3-knock-in mice (apoE3-BBB model). Consistent with the

* This work was supported, in whole or in part, by Grants-in-aid for Scientific Research (B) 19300138 and 21300145 from the Ministry of Education, Culture, Sports, Science, and Technology of Japan (to M. M.), a grant from the Ministry of Health, Labor, and Welfare of Japan (Research on Dementia, Health and Labor Sciences Research Grant H20-007) (to M. M.), Research Funding for Longevity Sciences Grant 21-11 from the National Center for Geriatrics and Gerontology, Japan (to M. M.), National Institutes of Health Grants R01AG027924 and R01AG035355 (to G. B.), and a Zenith Fellows award from the Alzheimer Association (to G. B.).

¹ To whom correspondence should be addressed: Dept. of Alzheimer's Disease Research, National Center for Geriatrics and Gerontology, 35 Gengo, Morioka, Obu, Aichi 474-8511, Japan. Tel.: 81-562-46-2311; Fax: 81-562-46-8569; E-mail: michi@ncgg.go.jp.

² The abbreviations used are: apoE, apolipoprotein E; A β , amyloid β ; AD, Alzheimer disease; BBB, blood-brain barrier; CM, conditioned medium; LDLR, LDL receptor; LRP, low density lipoprotein receptor-related protein; mBEC, mouse brain endothelial cell; RAP, receptor-associated protein; TEER, transendothelial electric resistance; TJ, tight junction.

results of *in vitro* studies, BBB permeability was higher in apoE4-knock-in mice than in apoE3-knock-in mice.

EXPERIMENTAL PROCEDURES

Materials—A mouse monoclonal anti-LDL receptor-related protein 1 (LRP1) antibody, a rabbit polyclonal anti-LDL receptor antibody, a rabbit monoclonal anti-very low-density lipoprotein (VLDL) receptor antibody, and an anti-phosphorylated PKC η (pPKC η) antibody were purchased from Abcam Inc. (Cambridge, MA). A mouse monoclonal anti-occludin antibody was purchased from Invitrogen, and a rabbit polyclonal anti-actin antibody was from Sigma. A goat polyclonal anti-apoE antibody was purchased from Millipore (Billerica, MA). Anti-phosphorylated Tyr (Tyr(P)), anti-phosphorylated Thr (Thr(P)), and rabbit polyclonal anti-PKC η antibodies were purchased from Santa Cruz Biotechnology (Santa Cruz, CA). Mouse control IgG was from Millipore Corp. (Bedford, MA), and rabbit control IgG was from Southern Biotech (Birmingham, AL). Recombinant receptor-associated protein (RAP) was produced and purified as described previously (22, 23).

Animals—Mice expressing human apoE were generated by the gene-targeting technique taking advantage of homologous recombination in embryonic stem cells (knock-in) (24). Three-week-old C57BL/6 mice were purchased from SLC Inc. (Hamamatsu, Japan). For astrocyte culture, pregnant C57BL/6 mice were purchased from SLC Inc., and newborn mice at postnatal day 2 were used for the experiment. ApoE-KO mice were obtained from the Jackson Laboratories (Bar Harbor, ME). The National Center for Geriatrics and Gerontology Institutional Animal Care and Use Committee approved the animal studies.

Evans Blue Assay—BBB permeability was quantified using the established Evans blue dye technique. Two hundred microliters of 20% mannitol (Sigma) was injected into 6-month-old apoE knock-in mice through the tail vein. After 30 min, 200 μ l of 2% Evans blue (Sigma) was injected intraperitoneally. Mice were killed at 3 h after injection. The cerebellum and cerebral cortex were collected and then incubated in 500 μ l of formamide for 72 h in the dark. Subsequently, the absorption (*A*) of the extracted dye was measured at 630 nm by spectrophotometry.

Cell Cultures—Primary cultures of mouse brain capillary endothelial cells (mBECs) were prepared from 3-week-old mice in accordance with the method described previously (21). The mice were killed, and the gray matter was dissected out. The gray matter was minced in ice-cold Dulbecco's modified Eagle's medium (DMEM) (Invitrogen) and then dissociated into single cells by 25 times of up- and down-strokes with a 5-ml pipette in 10 ml of DMEM containing 100 μ l of collagenase type 2 (100 mg/ml; Sigma), 150 μ l of DNase I (1 mg/ml; Roche Applied Science) followed by digestion for 1.5 h at 37 °C. The digest in 20% bovine serum albumin (BSA) (Sigma) in DMEM was centrifuged at 1,000 \times *g* for 20 min to obtain cell pellets. The microvessels obtained from the pellets were further digested with collagenase and dispase (1 mg/ml; Roche Applied Science) for 1 h at 37 °C. Microvessel endothelial cell clusters were separated on a 33% continuous Percoll (Pharmacia) gradient, collected, and washed twice in DMEM before plating on 60-mm plastic dishes coated with collagen type IV (Nitta Gelatin) and fibronectin (Calbiochem) (both 0.1 mg/ml). mBEC cultures

were maintained at 37 °C for 2 days in DMEM/F12 (Invitrogen) supplemented with mBEC medium I containing 10% FBS, basic fibroblast growth factor (1.5 ng/ml; Roche Applied Science), heparin (100 μ g/ml; Sigma), insulin (5 μ g/ml; Sigma), transferrin (5 μ g/ml; Sigma), sodium selenite (5 ng/ml; Sigma) (insulin-transferrin-sodium selenite media supplement), penicillin, streptomycin (Invitrogen), and puromycin (4 μ g/ml; Sigma). On the 3rd day, the medium was replaced with a new medium that contained all of the components of mBEC medium I except puromycin (mBEC medium II). When the cultures reached 80% confluence (4th day *in vitro*), the purified endothelial cells were passaged and used. Pure cultures of mouse cerebral pericytes were obtained by a 2-week culture of isolated brain microvessel fragments, which contain pericytes beside endothelial cells. When the cultures reached confluence, cells were treated with trypsin (Invitrogen), replated onto uncoated dishes, and cultured in DMEM supplemented with 10% FBS. Culture medium was changed every 3 days. Highly astrocyte-rich cultures were prepared in accordance with a method described previously (25). In brief, brains of day 2 postnatal human apoE-knock-in mice, WT mice, or apoE-KO mice were removed under anesthesia. The cerebral cortices from the mice were dissected, freed from meninges, and diced into small pieces; the cortical fragments were incubated in 0.25% trypsin and 20 mg/ml DNase I in PBS at 37 °C for 20 min. The fragments were then dissociated into single cells by pipetting. The cells were seeded in 75-cm² dishes with DMEM-containing 10% FBS at a density of 5 \times 10⁷ cells/dish. After 10 days of incubation *in vitro*, flasks were shaken at 37 °C overnight, and the remaining astrocytes in the monolayer were trypsinized (0.1%) and reseeded. The astrocyte-rich cultures were maintained in DMEM-containing 10% FBS until use.

Construction of *In Vitro* BBB Models—To construct *in vitro* models of BBB, pericytes (1.5 \times 10⁴ cells/cm²) were seeded on the bottom side of the polyester membrane of the Transwell inserts (Corning Inc., Corning, NY) coated with collagen type IV and fibronectin. The cells were allowed to adhere firmly overnight, then endothelial cells (1.5 \times 10⁵ cells/cm²) were seeded on the upper side of the inserts placed in the wells of 24-well culture plates (for measurement of TEER) or 6-well plates (for Western blotting). Astrocytes (1 \times 10⁵ cells/cm²) on the 6-well plates or 24-well plates were maintained in mBEC medium II. Finally, the Transwell inserts with mBECs and pericytes were placed into the 6-well or 24-well plates with astrocytes and maintained for 7 days. For the experiment to examine the effect of apoE-containing medium on BBB integrity, the double co-cultured model using pericytes and mBECs in the absence of astrocytes was used. For the preparation of conditioned media, primary astrocytes prepared from apoE3- or apoE4-knock-in mice were cultured in mBEC medium II for 48 h, and the conditioned media of apoE3-expressing astrocytes (apoE3-CM) or apoE4-expressing astrocytes (apoE4-CM) were collected. To determine the effect of apoE3-CM or apoE4-CM on BBB integrity, each CM was added only to the luminal side of the double co-cultured model, and the abluminal side was filled with mBEC medium II. These culture media were replaced with newly prepared CM or fresh mBEC medium II on the 3rd and 5th days, and TEER was determined on the 7th day.

ApoE Regulates Tight Junctions

Measurement of TEER—Barrier integrity in *in vitro* BBB models was analyzed by measurement of TEER. TEER was measured using an epithelial-volt-ohm meter and Endohm-24 chamber electrodes (World Precision Instruments). TEER of coated but cell-free filters was subtracted from the measured TEERs of models shown as $\Omega \times \text{cm}^2$.

Real-time PCR Analysis—The mRNA levels of TJ proteins were evaluated by real-time PCR analysis. Total RNA was extracted using a CellAmpTM Direct RNA Prep kit (Takara Bio Inc., Shiga, Japan) and reverse-transcribed with oligo(dT) and random primers using a PrimeScript RT reagent kit (Takara Bio Inc.). Relative real-time PCR was carried out using SYBR Premix Ex TaqTM II (Takara Bio Inc.) and Thermal Cycler Dice Real-time system TP-800 (Takara Bio Inc.) in accordance with the manufacturer's protocols. The oligonucleotide sequences used for the primer sets were 5'-GCTTATCTTGGGAGCCTGGACA-3' and 5'-GTCATTGCTTGGTGCATAATGATTG-3' for occludin, 5'-CACCACTACCAGCAGTCGATAA-3' and 5'-GTGTCGTCTGTCCACCATCTGGAA-3' for claudin 3, 5'-AGTTAAGGCACGGGTAGCACTCAC-3' and 5'-CAACGATGTTGGCGAACCAG-3' for claudin 5, and 5'-GCCAATCACAATTGCGAAGATG-3' and 5'-GCCACTCGAGCTGATCTGTCAC-3' for apoE.

Western Blotting—The protein expression levels of occludin, PKC η , and phosphorylated PKC η in *in vitro* BBB models were determined by Western blotting. Cells were washed with PBS three times, harvested using a cell scraper, and lysed by sonication in radioimmunoprecipitation assay buffer (1% Nonidet P-40, 0.5% sodium deoxycholate, 0.1% SDS, 150 mM NaCl, 50 mM Tris-HCl (pH 8.0), 1 mM EDTA). Cell lysates were subjected to SDS-PAGE with 7.5% gels (WAKO Pure Chemicals, Osaka, Japan) and transferred to polyvinylidene difluoride membranes (Millipore). The membrane was blotted with a primary antibody followed by a horseradish peroxidase-labeled secondary antibody (Cell Signaling Technology, Inc., Beverly, MA). The blot was developed using chemiluminescent substrate ECL Plus (GE Healthcare). Signals were visualized and quantified using a LAS-3000 miniluminescent image analyzer (Fujifilm, Tokyo, Japan). The protein level in cell lysates was normalized to the expression level of the actin protein. The phosphorylation state of occludin was analyzed by immunoprecipitation. For immunoprecipitation, cell lysates were incubated with magnetic protein G beads (Dynal, Hamburg, Germany) linked with an anti-Thr(P) or anti-Tyr(P) antibody. The obtained precipitates were washed three times with PBS and incubated at 70 °C for 10 min in SDS sample buffer. Dissociated occludin in the supernatant was analyzed by Western blotting as described above.

Statistical Analyses—The collected data were analyzed by one-way analysis of variance (ANOVA) including appropriate variables followed by Dunnett's test or unpaired Student's *t* test (comparison between two groups). Results were considered significant when $p < 0.05$.

RESULTS

BBB Integrity Was Impaired in ApoE4-BBB Model—First, we examined whether mBECs and primary pericytes express apoE. We confirmed that the mRNA level of apoE in mBECs was

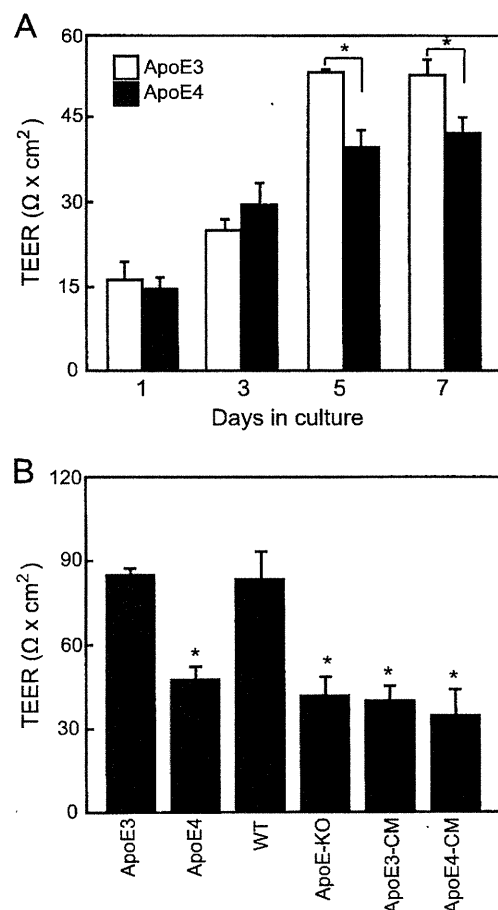


FIGURE 1. TEER in apoE3-BBB, apoE4-BBB, WT-BBB, and apoE-KO-BBB models. A, triple co-culture BBB models were prepared by using primary pericytes and mBECs from WT mouse brains and primary astrocytes from human apoE3- or apoE4-knock-in mice and were cultured for 7 days. TEER was measured on the indicated culture days and presented as $\Omega \times \text{cm}^2$. The data presented are means \pm S.D. (error bars) ($n = 3$). *, $p < 0.001$ compared with the values of apoE3-BBB models on day 7 or day 5 (unpaired Student's *t* test). B, triple co-culture BBB models were prepared by using primary pericytes and mBECs from WT mouse brains and primary astrocytes from human apoE3- or apoE4-knock-in mice, WT mice, or apoE-KO mice and were cultured for 7 days. To determine the effect of the apoE-containing conditioned media, double co-culture model using primary pericytes and mBECs in the absence of astrocytes was used. The conditioned media (48 h) from apoE3-expressing astrocytes (apoE3-CM) or apoE4-expressing astrocytes (apoE4-CM) were added only to the luminal side of double co-culture models and maintained for 7 days. Then, TEER was measured, and the values are presented as $\Omega \times \text{cm}^2$. The data presented are means \pm S.D. ($n = 3$). *, $p < 0.05$ versus apoE3-BBB model.

about 1,000 times lower than that in primary astrocytes (data not shown), and we did not detect apoE in the culture media of mBECs and primary pericytes by Western blotting (data not shown). Thus, we prepared mBECs and primary pericytes from wild-type mice and astrocytes from apoE3- or apoE4-knock-in mice, WT mice, and apoE-KO mice for the preparation of an *in vitro* BBB model. TEER increased in a manner that depended on the number of days of culture after preparing the *in vitro* BBB model and was significantly lower in the apoE4-BBB model than in the apoE3-BBB model on days 5 and 7 (Fig. 1A). We also evaluated TEER in *in vitro* BBB models with astrocytes prepared from WT mice, expressing endogenous mouse apoE, and astrocytes prepared from apoE-KO mice. We found that TEER

in the WT-BBB model was comparable with that in the apoE3-BBB model, whereas TEER in the apoE-KO-BBB model was significantly lower than that in the apoE3-BBB model (Fig. 1B). Furthermore, we performed experiments to determine the effect of apoE-containing media on BBB integrity. The conditioned media of primary astrocytes expressing apoE3 (apoE3-CM) or apoE4 (apoE4-CM) were added to the luminal side of the co-culture model with pericytes and mBECs in the absence of astrocytes. TEER was significantly lower in these models than in the apoE3-BBB model (Fig. 1B).

ApoE Isoforms Do Not Affect Expression Levels of TJ Proteins—Next, we analyzed the expression levels of occludin, claudin 3, and claudin 5, all of which were reported to be major constituents of TJ strands (15). Each BBB model was cultured for 7 days, and the mRNA levels of these proteins in mBECs were analyzed by real-time PCR. Results are shown as relative ratios to actin. The expression levels of occludin (Fig. 2A), claudin 3, and claudin 5 (data not shown) in the apoE3-BBB model were comparable with those in the apoE4-BBB, WT-BBB, and apoE-KO-BBB models.

Thr Phosphorylation of Occludin Was Regulated in an ApoE Isoform-dependent Manner—The phosphorylation of occludin at Tyr residues is reported to negatively regulate TJ integrity (26) whereas phosphorylation at Thr residues is required for the assembly of occludin into TJs (19). We then determined whether the phosphorylation of occludin is regulated in an apoE isoform-dependent manner. On day 7, mBECs were harvested using a cell scraper, and the level of phosphorylated occludin was determined by immunoprecipitation followed by Western blotting. We did not detect the phosphorylation of occludin at Tyr residues (data not shown). The levels of phosphorylated occludin at Thr residues were significantly lower in the apoE4-BBB model than in the apoE3-BBB model (Fig. 2B). The phosphorylated occludin at Thr residues was abolished in the apoE-KO-BBB model, whereas the level of phosphorylated occludin in the WT-BBB model was similar to that in the apoE3-BBB model (Fig. 2B). Consistent with the results of real-time PCR analysis, the protein level of occludin in the apoE3-BBB model was comparable with those in the apoE4-BBB, WT-BBB, and apoE-KO-BBB models (Fig. 2B). Recently, it has been reported that PKC η regulates the phosphorylation of occludin at Thr residues in epithelial TJs (19). We then analyzed the activation states of PKC η in the *in vitro* BBB models. On day 7, mBECs in the BBB models were harvested, lysed, and subjected to SDS-PAGE followed by immunoblotting with the antibody specific for phosphorylated PKC η at the Ser-674 residue, which is an activated form of PKC η (27). As shown in Fig. 2C, phosphorylation of PKC η was significantly attenuated in the apoE4-BBB model compared with the apoE3-BBB model, indicating that apoE isoforms differentially influence the activation of PKC η . The level of phosphorylated PKC η was significantly lower in the apoE-KO-BBB model than in the apoE3-BBB model, and the level of phosphorylated PKC η in the WT-BBB model was comparable with that in the apoE3-BBB model (Fig. 2C). We examined the phosphorylation of other PKC isoforms, PKC δ and PKC ζ , which interact directly with TJs (17), and found no significant difference in the levels of phosphorylated PKC isoforms (data not shown).

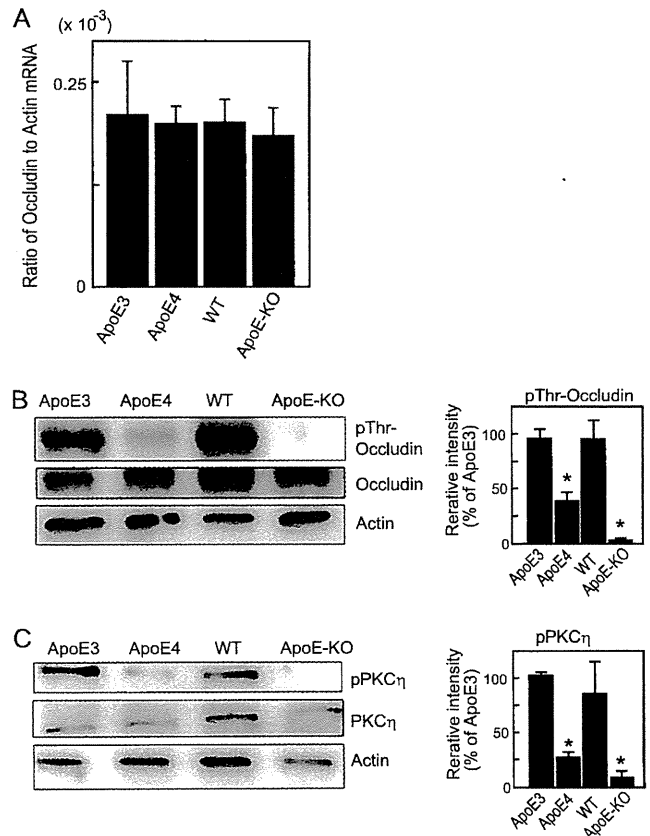


FIGURE 2. Phosphorylation of occludin and PKC η in mBECs of apoE3-BBB, apoE4-BBB, WT-BBB, and apoE-KO-BBB models. A, triple co-culture BBB models were prepared by using primary pericytes and mBECs from WT mouse brains and primary astrocytes from human apoE3 or apoE4 knock-in mice, WT mice, or apoE-KO mice and were cultured for 7 days. Total RNA of mBECs was collected. Relative real-time PCR analysis was performed to compare the expression levels of occludin. Results are shown as relative ratios to actin. The data presented are means \pm S.D. (error bars) ($n = 3$). B, triple co-cultured models were cultured for 7 days. On day 7, mBECs were harvested, and the obtained cell lysates were subjected to immunoprecipitation and Western blotting. For the detection of occludin phosphorylated at its Thr residues, immunoprecipitation with the anti-Thr(P) antibody followed by immunoblotting with the anti-occludin antibody was performed. For the detection of total occludin, cell lysates were subjected to SDS-PAGE followed by probing with the anti-occludin antibody. The anti- β actin antibody was used as the loading control. The graph shows the levels of phosphorylated occludin at Thr residues and total occludin. The data presented are means \pm S.D. ($n = 3$). *, $p < 0.001$ versus apoE3-BBB model. C, triple co-cultured models were cultured for 7 days. On day 7, mBECs were harvested, and the obtained cell lysates were subjected to Western blotting with the anti-phosphorylated PKC η and anti-PKC η antibodies. The graph shows the levels of phosphorylated and total pPKC η . The data presented are means \pm S.D. ($n = 3$). *, $p < 0.001$ versus apoE3-BBB model.

LRP1 Is Involved in the Regulation of the TJ Integrity in the ApoE3-BBB Model—ApoE is a ligand for receptors of the LDL receptor (LDLR) superfamily, several of which act both as endocytic receptors (28) and signaling receptors (5). Thus, we examined the effect of the RAP on the phosphorylation of PKC η . RAP, a 39-kDa protein, is a specialized chaperone of members of the LDLR family, including LRP1 (29, 30). RAP binds to LRP1 at multiple sites (29, 30) with high affinity ($K_D = 1-10$ nM) (31). RAP has also been used extensively as an antagonist of LRP1 (32). On day 7, RAP (1 μ M) was added to the media of astrocytes in an *in vitro* BBB model and cultured for 4 h at 37 $^{\circ}$ C. After

ApoE Regulates Tight Junctions

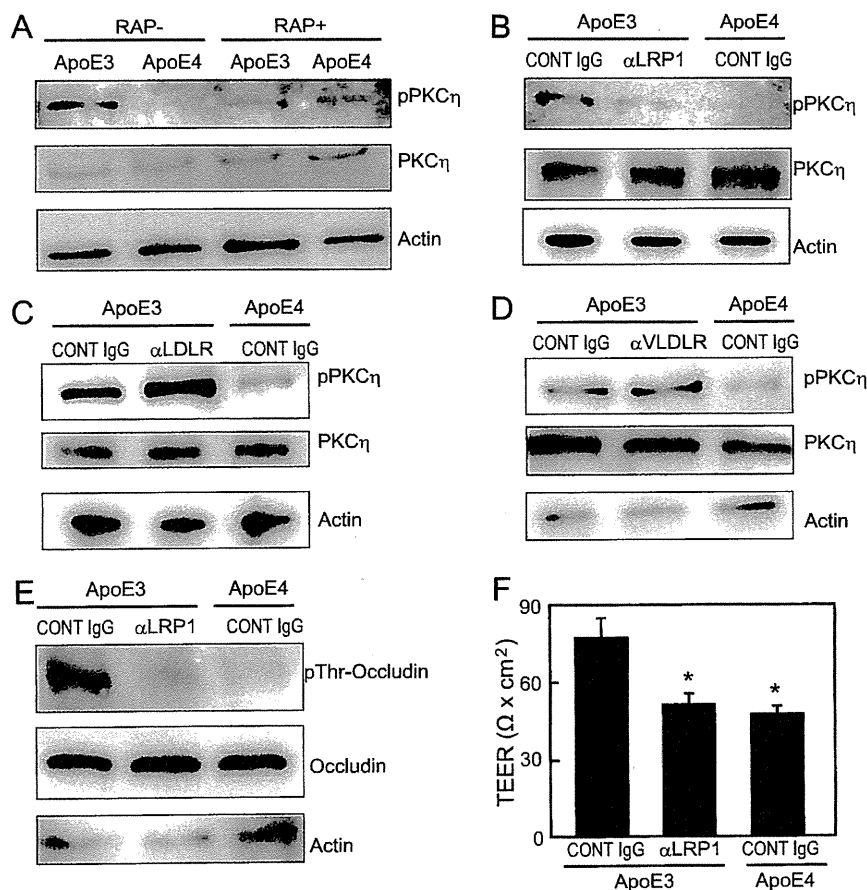


FIGURE 3. LRP1 is involved in the regulation of TJ integrity in the apoE3-BBB model. *A–D*, apoE3- and apoE4-BBB models were cultured for 7 days. On day 7, the *in vitro* BBB models were treated with RAP (*A*) (1 μ M) or the anti-LRP1 (*B*), anti-LDLR (*C*), or anti-VLDLR antibody (*D*) (25 μ g/ml) for 4 h at 37 °C. After treatment, mBECs were harvested using a cell scraper, and the obtained cell lysates were subjected to Western blotting using anti-phosphorylated PKC η and anti-PKC η antibodies. *E*, apoE3- and apoE4-BBB models were cultured for 7 days. On day 7, the *in vitro* BBB models were treated with the anti-LRP1 antibody or isotype IgG (25 μ g/ml) for 4 h at 37 °C. After treatment, mBEC lysates were immunoprecipitated with the polyclonal anti-Thr(P) antibody, and the immunoprecipitates were subjected to Western blotting using the anti-occludin antibody or anti-phosphooccludin antibody. *F*, apoE3- and apoE4-BBB models were cultured for 7 days and then treated with the anti-LRP1 antibody or isotype IgG (25 μ g/ml) for 4 h at 37 °C. After treatment, TEER was measured, and the values are presented as $\Omega \times \text{cm}^2$. The data presented are means \pm S.D. (error bars) ($n = 3$). *, $p < 0.005$ compared with the values of apoE3-BBB models treated with control IgG (Dunnett's test).

incubation, the phosphorylation of PKC η in mBECs was analyzed by Western blotting. The treatment of the apoE3-BBB model with RAP attenuated the phosphorylation of PKC η to a level similar to that of the apoE4-BBB model (Fig. 3*A*). Because RAP inhibits LRP1 as well as the LDLR (29) and because apoE-containing particles can bind to the very low-density lipoprotein (VLDL) receptor (33), we next treated the apoE3-BBB model with the anti-LRP1, anti-LDLR, or anti-VLDLR antibody (25 μ g/ml), which recognizes the extracellular domain of LRP1, LDLR, or VLDLR, respectively, on day 7 for 4 h at 37 °C to determine whether specific apoE receptors are involved in PKC η phosphorylation. Among these antibodies, only the anti-LRP1 receptor antibody suppressed the phosphorylation of PKC η (Fig. 3, *B–D*). Consistent with this suppression of PKC η phosphorylation, the treatment of the apoE3-BBB model with the anti-LRP1 antibody also suppressed the phosphorylation of occludin at Thr residues (Fig. 3*E*). Next, we examined whether treatment of the apoE3-BBB model with the anti-LRP1 antibody impairs TJ integrity. The prepared apoE3-BBB model was cultured for 7 days, and the anti-LRP1 antibody (25 μ g/ml) was added to the astrocyte culture medium. After further incuba-

tion of the cultures for 4 h at 37 °C, TJ integrity was evaluated by measuring TEER. Treatment of the apoE3-BBB model with the anti-LRP1 antibody significantly decreased TEER (Fig. 3*F*), indicating that TJ integrity requires the function of apoE receptor LRP1.

BBB Integrity Is Impaired in ApoE4-knock-in Mice—Finally, we evaluated the BBB integrity in human apoE3-, apoE4-knock-in mice, and apoE-KO mice. BBB integrity was evaluated using an Evans blue dye technique. Consistent with the results shown in Fig. 1, BBB integrity was impaired in the apoE4-knock-in mice compared with the apoE3-knock-in mice (Fig. 4). Consistent with previous studies (9, 11), BBB integrity was impaired in the apoE-KO mice (Fig. 4). We found a higher amount of leakage in the cerebellum of human apoE-knock-in mice than in the cerebrum, which is consistent with the findings of previous studies using apoE-KO mice (9, 11).

DISCUSSION

In this report, we provided evidence that TEER is lower in the apoE4-BBB and apoE-KO models than in the apoE3-BBB and WT-BBB models. The activation of PKC η and the phosphory-

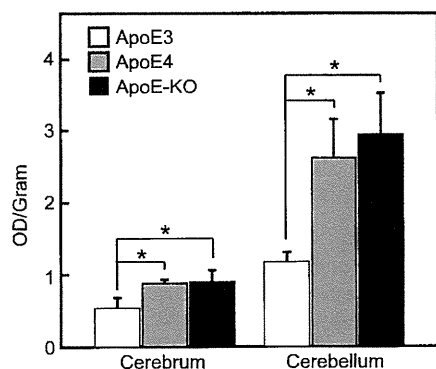


FIGURE 4. **BBB integrity is impaired in apoE4-knock-in mice.** The BBB integrity in apoE3-knock-in mice, apoE4-knock-in mice, and apoE-KO mice was evaluated using an Evans blue dye technique. Two hundred microliters of 20% mannitol was injected through the tail vein. Thirty minutes after injection, 200 μ l of 2% Evans blue dye was injected intraperitoneally. The distribution of the dye was confirmed by a visible change in the color of the skin within 1 h after injection. Three hours after the injection, the mice were killed, and their brains were removed. The cerebrum and cerebellum were immediately collected, weighed, and incubated in 500 μ l of formamide for 72 h at room temperature in the dark. The absorbance of the extracted dye was measured at 630 nm. The data presented are means \pm S.D. (error bars) ($n = 3$). *, $p < 0.05$.

lation of occludin at its Thr residues, which regulates TJ integrity, were dependent on the apoE isoform. Furthermore, the treatment of the apoE3-BBB model with the anti-LRP1 antibody diminished the activation of PKC η and phosphorylation of occludin, suggesting that LRP1 may be involved in the regulation of TJ integrity through the activation of PKC η and phosphorylation of occludin at its Thr residues in the apoE3-BBB model. Our results also indicate that this pathway is impaired in the apoE4-BBB model. Consistent with the results of *in vitro* studies, BBB permeability was increased in the apoE4-knock-in mice and apoE-KO mice compared with the apoE3-knock-in mice. As revealed in previous studies (7, 8), astrocytes are involved in the control of BBB integrity. Astrocytes are considered to be the major source of apoE in the CNS (4–6), and apoE deficiency leads to BBB leakage (9–11). These lines of evidence suggest that astrocytes may regulate BBB integrity through apoE. In the present study, our findings indicate that apoE secreted from astrocytes is involved in the regulation of TJ integrity through the activation of PKC η and phosphorylation of occludin at its Thr residues in an LRP1-mediated manner in the apoE3-BBB model and that this pathway is impaired in the apoE4-BBB model. We provide the first evidence that TJ integrity in BBB is regulated in an apoE isoform-dependent manner.

ApoE-containing particles act as ligands of LDLR family members such as LRP1 and play critical roles in maintaining brain lipid homeostasis and associated synaptic and neuronal integrity (4, 34). Previous studies have shown that apoE induces lipid release to generate HDL-like particles from macrophages and astrocytes in an isoform-dependent manner; apoE3 induces a greater lipid release than apoE4 (35–39). In addition to functioning as lipid carriers, a recent study showed that apoE3-containing particles act as signaling molecules through LRP1 to activate PKC δ , a novel PKC isoform (40), and protect neurons from apoptosis in an apoE isoform-dependent manner (41). Here, we showed that apoE regulates the activation of PKC η , which is also a novel PKC isoform (40), through LRP1 in

mBECs in the *in vitro* BBB model. Thus, our results suggest that apoE-containing particles also act as signaling molecules to regulate the activation of PKC η , the subsequent phosphorylation of occludin at its Thr residues, and TJ integrity. Our findings also indicate that apoE4-containing particles might be less efficient as signaling molecules than apoE3-containing particles.

ApoE4 is a major risk factor for AD. Although how apoE4 influences AD onset and progression has not been fully understood yet, recent studies suggest that the differential effects of apoE isoforms on amyloid- β (A β) aggregation and clearance could play important roles in AD pathogenesis. Human apoE-transgenic mice display an isoform-specific pattern of A β deposition (E3 < E4) (42–46). Previous studies have shown that lipid-poor apoE4 and lipid-free apoE4 enhance A β production by increasing LRP1- and apoER2-mediated endocytosis of an amyloid precursor protein (47, 48). ApoE also facilitates the proteolytic clearance of A β from the brain in an apoE isoform-dependent manner and requires its lipidation (49). Considering BBB as a pathway of A β clearance in the brain (50–52), a recent study has shown that A β complexed to apoE2 and apoE3 is cleared out of the brain at a significantly higher rate than A β complexed to apoE4 (53). Interestingly, several studies have demonstrated that there is an increased permeability in the BBB of the AD model mice compared with age-matched control mice (54, 55) and that A β fibrils could increase the permeability of bovine pulmonary arterial endothelial cells, as detected by TEER measurement (56). Furthermore, a recent study using pericyte-deficient mice has shown that BBB breakdown is associated with the accumulation of neurotoxic and/or vasculotoxic serum proteins in the brain, which leads to secondary neurodegenerative changes (57). In this study, we provide evidence that TJ integrity in BBB is impaired in the apoE4-BBB model and apoE4-knock-in mice. Thus, these lines of evidence suggest that apoE4 may affect AD pathogenesis and/or neurodegeneration through its effects on BBB. We have shown using *in vitro* and *in vivo* models that apoE regulates the activation of PKC η , the phosphorylation of occludin at Thr residues, and TJ integrity in an apoE isoform-dependent manner. Further study will be needed to elucidate the contribution of BBB impairment to AD pathogenesis.

REFERENCES

- Mahley, R. W. (1988) *Science* **240**, 622–630
- Corder, E. H., Saunders, A. M., Strittmatter, W. J., Schmechel, D. E., Gaskell, P. C., Small, G. W., Roses, A. D., Haines, J. L., and Pericak-Vance, M. A. (1993) *Science* **261**, 921–923
- Saunders, A. M., Strittmatter, W. J., Schmechel, D., George-Hyslop, P. H., Pericak-Vance, M. A., Joo, S. H., Rosi, B. L., Gusella, J. F., Crapper-McLachlan, D. R., Alberts, M. J., et al. (1993) *Neurology* **43**, 1467–1472
- Bu, G. (2009) *Nat. Rev. Neurosci.* **10**, 333–344
- Herz, J., and Bock, H. H. (2002) *Annu. Rev. Biochem.* **71**, 405–434
- Herz, J., and Chen, Y. (2006) *Nat. Rev. Neurosci.* **7**, 850–859
- Janzer, R. C., and Raff, M. C. (1987) *Nature* **325**, 253–257
- Rubin, L. L., and Staddon, J. M. (1999) *Annu. Rev. Neurosci.* **22**, 11–28
- Hafezi-Moghadam, A., Thomas, K. L., and Wagner, D. D. (2007) *Am. J. Physiol. Cell Physiol.* **292**, C1256–1262
- Methia, N., Andr e, P., Hafezi-Moghadam, A., Economopoulos, M., Thomas, K. L., and Wagner, D. D. (2001) *Mol. Med.* **7**, 810–815
- Fullerton, S. M., Shirman, G. A., Strittmatter, W. J., and Matthew, W. D. (2001) *Exp. Neurol.* **169**, 13–22
- Reese, T. S., and Karnovsky, M. J. (1967) *J. Cell Biol.* **34**, 207–217

ApoE Regulates Tight Junctions

13. Hori, S., Ohtsuki, S., Hosoya, K., Nakashima, E., and Terasaki, T. (2004) *J. Neurochem.* **89**, 503–513
14. Tao-Cheng, J. H., Nagy, Z., and Brightman, M. W. (1987) *J. Neurosci.* **7**, 3293–3299
15. Tsukita, S., and Furuse, M. (1999) *Trends Cell Biol.* **9**, 268–273
16. Basuroy, S., Sheth, P., Kuppuswamy, D., Balasubramanian, S., Ray, R. M., and Rao, R. K. (2003) *J. Biol. Chem.* **278**, 11916–11924
17. Helfrich, I., Schmitz, A., Zigrino, P., Michels, C., Haase, I., le Bivic, A., Leitges, M., and Niessen, C. M. (2007) *J. Invest. Dermatol.* **127**, 782–791
18. Stuart, R. O., and Nigam, S. K. (1995) *Proc. Natl. Acad. Sci. U.S.A.* **92**, 6072–6076
19. Suzuki, T., Elias, B. C., Seth, A., Shen, L., Turner, J. R., Giorgianni, F., Desiderio, D., Guntaka, R., and Rao, R. (2009) *Proc. Natl. Acad. Sci. U.S.A.* **106**, 61–66
20. Abbott, N. J., Rönnbäck, L., and Hansson, E. (2006) *Nat. Rev. Neurosci.* **7**, 41–53
21. Nakagawa, S., Deli, M. A., Nakao, S., Honda, M., Hayashi, K., Nakaoka, R., Kataoka, Y., and Niwa, M. (2007) *Cell Mol. Neurobiol.* **27**, 687–694
22. Li, Y., Chen, J., Lu, W., McCormick, L. M., Wang, J., and Bu, G. (2005) *J. Cell Sci.* **118**, 5305–5314
23. Warshawsky, I., Bu, G., and Schwartz, A. L. (1993) *J. Clin. Invest.* **92**, 937–944
24. Hamanaka, H., Katoh-Fukui, Y., Suzuki, K., Kobayashi, M., Suzuki, R., Motegi, Y., Nakahara, Y., Takeshita, A., Kawai, M., Ishiguro, K., Yokoyama, M., and Fujita, S. C. (2000) *Hum. Mol. Genet.* **9**, 353–361
25. Michikawa, M., Gong, J. S., Fan, Q. W., Sawamura, N., and Yanagisawa, K. (2001) *J. Neurosci.* **21**, 7226–7235
26. Elias, B. C., Suzuki, T., Seth, A., Giorgianni, F., Kale, G., Shen, L., Turner, J. R., Naren, A., Desiderio, D. M., and Rao, R. (2009) *J. Biol. Chem.* **284**, 1559–1569
27. Redig, A. J., Sassano, A., Majchrzak-Kita, B., Katsoulidis, E., Liu, H., Altman, J. K., Fish, E. N., Wickrema, A., and Platanius, L. C. (2009) *J. Biol. Chem.* **284**, 10301–10314
28. Brown, M. S., and Goldstein, J. L. (1976) *Science* **191**, 150–154
29. Bu, G., and Marzolo, M. P. (2000) *Trends Cardiovasc. Med.* **10**, 148–155
30. Bu, G., Geuze, H. J., Strous, G. J., and Schwartz, A. L. (1995) *EMBO J.* **14**, 2269–2280
31. Iadonato, S. P., Bu, G., Maksymovitch, E. A., and Schwartz, A. L. (1993) *Biochem. J.* **296**, 867–875
32. Kanekiyo, T., and Bu, G. (2009) *J. Biol. Chem.* **284**, 33352–33359
33. Ruiz, J., Kouivaskaia, D., Migliorini, M., Robinson, S., Saenko, E. L., Gorlatova, N., Li, D., Lawrence, D., Hyman, B. T., Weisgraber, K. H., and Strickland, D. K. (2005) *J. Lipid Res.* **46**, 1721–1731
34. Liu, Q., Trotter, J., Zhang, J., Peters, M. M., Cheng, H., Bao, J., Han, X., Weeber, E. J., and Bu, G. (2010) *J. Neurosci.* **30**, 17068–17078
35. Hara, M., Matsushima, T., Satoh, H., Iso-o, N., Noto, H., Togo, M., Kimura, S., Hashimoto, Y., and Tsukamoto, K. (2003) *Arterioscler. Thromb. Vasc. Biol.* **23**, 269–274
36. Michikawa, M., Fan, Q. W., Isobe, I., and Yanagisawa, K. (2000) *J. Neurochem.* **74**, 1008–1016
37. Gong, J. S., Kobayashi, M., Hayashi, H., Zou, K., Sawamura, N., Fujita, S. C., Yanagisawa, K., and Michikawa, M. (2002) *J. Biol. Chem.* **277**, 29919–29926
38. Minagawa, H., Gong, J. S., Jung, C. G., Watanabe, A., Lund-Katz, S., Phillips, M. C., Saito, H., and Michikawa, M. (2009) *J. Neurosci. Res.* **87**, 2498–2508
39. Minagawa, H., Watanabe, A., Akatsu, H., Adachi, K., Ohtsuka, C., Terayama, Y., Hosono, T., Takahashi, S., Wakita, H., Jung, C. G., Komano, H., and Michikawa, M. (2010) *J. Biol. Chem.* **285**, 38382–38388
40. Steinberg, S. F. (2008) *Physiol. Rev.* **88**, 1341–1378
41. Hayashi, H., Campenot, R. B., Vance, D. E., and Vance, J. E. (2009) *J. Biol. Chem.* **284**, 29605–29613
42. Bales, K. R., Liu, F., Wu, S., Lin, S., Koger, D., DeLong, C., Hansen, J. C., Sullivan, P. M., and Paul, S. M. (2009) *J. Neurosci.* **29**, 6771–6779
43. Buttini, M., Yu, G. Q., Shockley, K., Huang, Y., Jones, B., Masliah, E., Mallory, M., Yeo, T., Longo, F. M., and Mucke, L. (2002) *J. Neurosci.* **22**, 10539–10548
44. Dolev, I., and Michaelson, D. M. (2004) *Proc. Natl. Acad. Sci. U.S.A.* **101**, 13909–13914
45. Fagan, A. M., Watson, M., Parsadonian, M., Bales, K. R., Paul, S. M., and Holtzman, D. M. (2002) *Neurobiol. Dis.* **9**, 305–318
46. Holtzman, D. M., Bales, K. R., Tenkova, T., Fagan, A. M., Parsadonian, M., Sartorius, L. J., Mackey, B., Olney, J., McKeel, D., Wozniak, D., and Paul, S. M. (2000) *Proc. Natl. Acad. Sci. U.S.A.* **97**, 2892–2897
47. He, X., Cooley, K., Chung, C. H., Dashti, N., and Tang, J. (2007) *J. Neurosci.* **27**, 4052–4060
48. Ye, S., Huang, Y., Müllendorff, K., Dong, L., Giedt, G., Meng, E. C., Cohen, F. E., Kuntz, I. D., Weisgraber, K. H., and Mahley, R. W. (2005) *Proc. Natl. Acad. Sci. U.S.A.* **102**, 18700–18705
49. Jiang, Q., Lee, C. Y., Mandrekar, S., Wilkinson, B., Cramer, P., Zelcer, N., Mann, K., Lamb, B., Willson, T. M., Collins, J. L., Richardson, J. C., Smith, J. D., Comery, T. A., Riddell, D., Holtzman, D. M., Tontonoz, P., and Landreth, G. E. (2008) *Neuron* **58**, 681–693
50. Bell, R. D., Deane, R., Chow, N., Long, X., Sagare, A., Singh, I., Streb, J. W., Guo, H., Rubio, A., Van Nostrand, W., Miano, J. M., and Zlokovic, B. V. (2009) *Nat. Cell Biol.* **11**, 143–153
51. Ito, S., Ohtsuki, S., Kamiie, J., Nezu, Y., and Terasaki, T. (2007) *J. Neurochem.* **103**, 2482–2490
52. Zlokovic, B. V. (2008) *Neuron* **57**, 178–201
53. Deane, R., Sagare, A., Hamm, K., Parisi, M., Lane, S., Finn, M. B., Holtzman, D. M., and Zlokovic, B. V. (2008) *J. Clin. Invest.* **118**, 4002–4013
54. Dickstein, D. L., Biron, K. E., Ujjiie, M., Pfeifer, C. G., Jeffries, A. R., and Jeffries, W. A. (2006) *FASEB J.* **20**, 426–433
55. Ujjiie, M., Dickstein, D. L., Carlow, D. A., and Jeffries, W. A. (2003) *Microcirculation* **10**, 463–470
56. Nagababu, E., Usatyuk, P. V., Enika, D., Natarajan, V., and Rifkin, J. M. (2009) *J. Alzheimers Dis.* **17**, 845–854
57. Bell, R. D., Winkler, E. A., Sagare, A. P., Singh, I., LaRue, B., Deane, R., and Zlokovic, B. V. (2010) *Neuron* **68**, 409–427

RESEARCH ARTICLE

Open Access

Extracellular and intraneuronal HMW-AβOs represent a molecular basis of memory loss in Alzheimer's disease model mouse

Ayumi Takamura^{1,2}, Yasuhide Okamoto^{1,3}, Takeshi Kawarabayashi², Tatsuki Yokoseki³, Masao Shibata³, Akihiko Mouri⁴, Toshitaka Nabeshima⁴, Hui Sun¹, Koji Abe⁵, Tsuneo Urisu⁶, Naoki Yamamoto¹, Mikio Shoji², Katsuhiko Yanagisawa¹, Makoto Michikawa¹, Etsuro Matsubara^{1,2*}

Abstract

Background: Several lines of evidence indicate that memory loss represents a synaptic failure caused by soluble amyloid β ($A\beta$) oligomers. However, the pathological relevance of $A\beta$ oligomers ($A\beta$ Os) as the trigger of synaptic or neuronal degeneration, and the possible mechanism underlying the neurotoxic action of endogenous $A\beta$ Os remain to be determined.

Results: To specifically target toxic $A\beta$ Os *in vivo*, monoclonal antibodies (1A9 and 2C3) specific to them were generated using a novel design method. 1A9 and 2C3 specifically recognize soluble $A\beta$ Os larger than 35-mers and pentamers on Blue native polyacrylamide gel electrophoresis, respectively. Biophysical and structural analysis by atomic force microscopy (AFM) revealed that neurotoxic 1A9 and 2C3 oligomeric conformers displayed non-fibrillar, relatively spherical structure. Of note, such $A\beta$ Os were taken up by neuroblastoma (SH-SY5Y) cell, resulted in neuronal death. In humans, immunohistochemical analysis employing 1A9 or 2C3 revealed that 1A9 and 2C3 stain intraneuronal granules accumulated in the perikaryon of pyramidal neurons and some diffuse plaques. Fluoro Jade-B binding assay also revealed 1A9- or 2C3-stained neurons, indicating their impending degeneration. In a long-term low-dose prophylactic trial using active 1A9 or 2C3 antibody, we found that passive immunization protected a mouse model of Alzheimer's disease (AD) from memory deficits, synaptic degeneration, promotion of intraneuronal $A\beta$ Os, and neuronal degeneration. Because the primary antitoxic action of 1A9 and 2C3 occurs outside neurons, our results suggest that extracellular $A\beta$ Os initiate the AD toxic process and intraneuronal $A\beta$ Os may worsen neuronal degeneration and memory loss.

Conclusion: Now, we have evidence that HMW- $A\beta$ Os are among the earliest manifestation of the AD toxic process in mice and humans. We are certain that our studies move us closer to our goal of finding a therapeutic target and/or confirming the relevance of our therapeutic strategy.

Background

Alzheimer's disease (AD) represents the so-called "storage disorder" of amyloid β ($A\beta$). The AD brain contains soluble and insoluble $A\beta$, both of which have been hypothesized to underlie the development of cognitive deficits or dementia [1-3]. The steady-state level of $A\beta$ is controlled by the generation of $A\beta$ from its precursor, the degradation of $A\beta$ within the brain, and transport of $A\beta$ out of the

brain. The imbalance among three metabolic pathways results in excessive accumulation and deposition of $A\beta$ in the brain, which may trigger a complex downstream cascade (e.g., primary amyloid plaque formation or secondary tauopathy and neurodegeneration) leading to memory loss or dementia in AD. Accumulated lines of evidence indicate that such a memory loss represents a synaptic failure caused directly by soluble $A\beta$ oligomers ($A\beta$ Os) [4-6], whereas amyloid fibrils may cause neuronal injury indirectly via microglial activation [7]. Thus, the classical amyloid cascade hypothesis [8] underwent a modification in which the emphasis is switched to the intermediate

* Correspondence: etsuro@cc.hirosaki-u.ac.jp

¹Department of Alzheimer's Disease Research, Research Institute, National Center for Geriatrics and Gerontology, Aichi, Japan

Full list of author information is available at the end of the article